Bioprinting 21 (2021) e00124

Contents lists available at ScienceDirect

Bioprinting

journal homepage: www.elsevier.com/locate/bprint

3D bioprinting for lung and tracheal tissue engineering: Criteria, advances, challenges, and future directions

Seyed Hossein Mahfouzi [a], Seyed Hamid Safiabadi Tali [a], Ghassem Amoabediny [a,b,*]

[a] Department of Biomedical Engineering, The Research Center for New Technologies in Life Science Engineering, University of Tehran, No. 4, Orouji all., 16 Azar St., P.O. Box: 11155-4563, Tehran, Iran

[b] Department of Biotechnology and Pharmaceutical Engineering, School of Chemical Engineering, College of Engineering, University of Tehran, No. 4, Orouji all., 16 Azar St., P.O. Box: 11155-4563, Tehran, Iran

ARTICLE INFO

Keywords:
Tissue engineering
3D bioprinting
Alveolar mimicking
Tracheal regeneration
Bioreactors

ABSTRACT

Transplantation is the only long-term treatment option for patients with end-stage lung and tracheal diseases. However, transplantation is limited by shortage of donor organs and post-implant tissue rejection. Lung and tracheal tissue engineering by 3D bioprinting is a promising approach to address these limitations with the ultimate goal of producing implantable lung and tracheal constructs. This paper aims to review the current state of 3D bioprinting technology for lung and tracheal tissue engineering. First, the criteria for engineering lungs and trachea via bioprinting are presented, covering scaffold design criteria, required biomechanical and biochemical features for bioinks, and appropriate bioprinting techniques. Then the ongoing progress of the field is reviewed, demonstrating great achievements in alveolar function mimicking and tracheal regeneration. Next, the remaining challenges and relevant potential solutions regarding printing of hierarchical vascularization and architecture are discussed. Finally, the use of a universal bioink with a focus on decellularized-extracellular matrix, pluripotent stem cells, stereolithography printing method, and automated monitoring bioreactors are presented as future directions to accelerate achieving functional 3D-printed lungs and trachea for transplantation.

1. Introduction

Over four million people die annually from respiratory diseases, and estimates show that chronic obstructive pulmonary disease (COPD) alone will become the third leading cause of death worldwide in 2030, according to the World Health Organization (WHO) [1,2]. Tissue transplantation is the only treatment option for patients with end-stage respiratory diseases; however, this option suffers from issues such as lack of donor organs and serious transplant-related risks, including blood clots, infections, and rejection of new implants. Therefore, researchers have focused on engineering lungs and trachea to create implantable tissues [3–5].

Among engineering approaches, producing synthetic, decellularized, and 3D-printed (3DP) scaffolds are the leading ones. Nevertheless, synthetic approaches such as the use of hydrogels in a bulk manner or electrospun scaffolds are not able to mimic the hierarchical structure of the lungs due to the low control over scaffold geometry, damage to encapsulated cells, and insufficient control of cell patterning [6–9]. Also, lung decellularization methods have major challenges such as vascular failure, insufficient cell ingrowth into decellularized lungs, and the inability to target the proper placement of the cells [10–12]. 3D bioprinting, however, due to the precise cell and material patterning, has received great attention recently [13–15]. 3D bioprinting technology allows for printing cells or biologically derived materials to create scaffolds and tissues with appropriate biochemical, biomechanical, and physiological properties with regard to patient-specific needs (Fig. 1A–C) [16]. Therefore, 3D bioprinting is a promising candidate to be used for producing complex structures of lungs and trachea. The hierarchical structure of the lungs consists of 23 generations on average, functionally dividing into the conducting portion (e.g., trachea and bronchi) and respiratory portion ending in alveoli where the gas exchange occurs (Fig. 1D) [17,18]. Recently, significant progress has been made in 3D bioprinting of both the conducting portion [19–22] and the respiratory portion [23]. Also, informative review papers have been published with a focus on the applications of 3D bioprinting in airway obstruction [24] and hollow organs [25]. However, no recent review paper has

* Corresponding author. Department of Biotechnology and Pharmaceutical Engineering, School of Chemical Engineering, College of Engineering, University of Tehran, No. 4, Orouji all., 16 Azar St., P.O. Box: 11155-4563, Tehran, Iran.
E-mail address: amoabediny@ut.ac.ir (G. Amoabediny).

https://doi.org/10.1016/j.bprint.2020.e00124
Received 7 September 2020; Received in revised form 14 December 2020; Accepted 14 December 2020

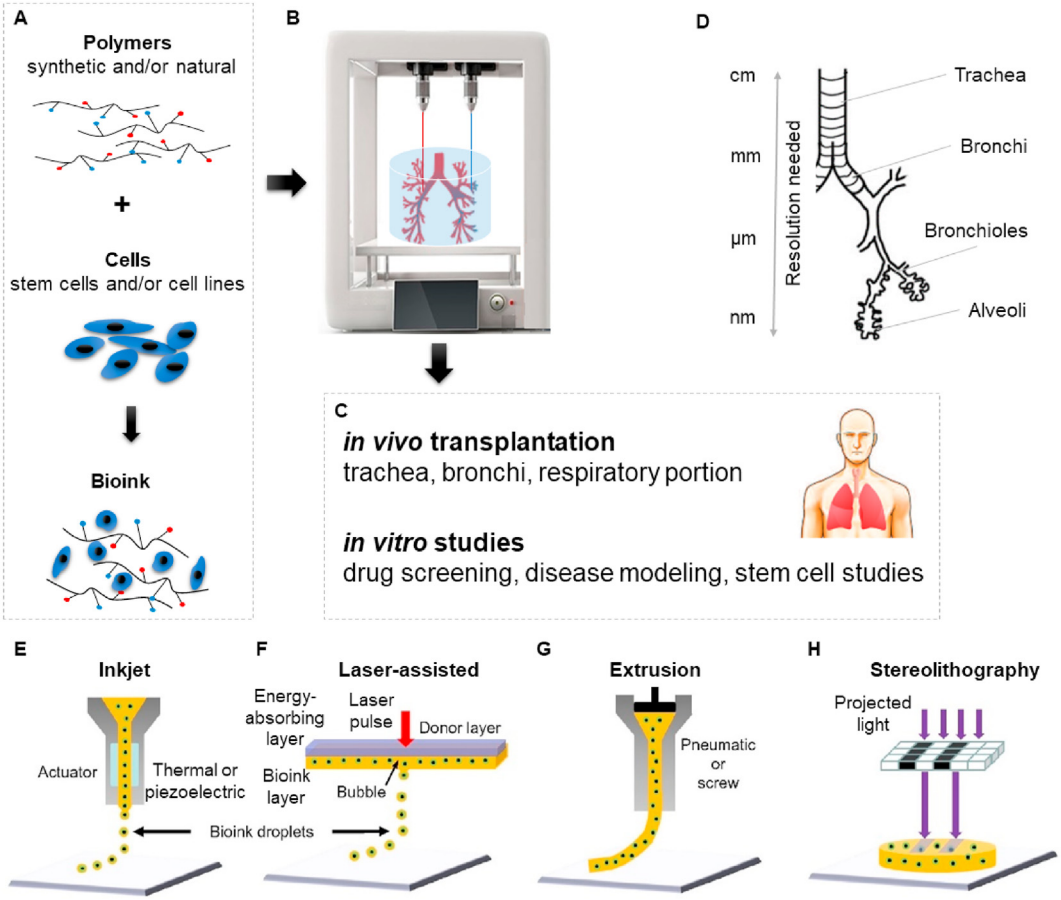

Fig. 1. Schematic of 3D bioprinting of lungs and trachea using bioinks in a bioprinter. (**A–C**) Bioprinting process and applications. **(A)** Bioinks are created by combining various synthetic and/or natural polymers and stem cells and/or cell lines. **(B)** Bioprinters use bioinks to produce functional 3D-printed (3DP) constructs. **(C)** 3DP constructs can be transplanted into patients and also can be used for drug screening, disease modeling, and *in vitro* stem cell studies. **(D)** Schematic of the lung showing the required resolutions for bioprinting different parts of a lung tissue. **(E–H)** Simplified illustrations of 3D bioprinting types. **(E)** Inkjet printers eject small droplets of the bioink sequentially to construct tissues. **(F)** Laser-assisted printers use a laser to vaporize a region in the donor layer forming a bubble that drives the suspended bioink to fall onto the substrate. **(G)** Extrusion printers use pneumatics or mechanical pressure to continuously extrude a highly viscous bioink. **(H)** Stereolithographic printers use a digital light projector to selectively crosslink bioinks plane-by-plane. (E–H) reproduced/adapted with permission from Ref. [47].

comprehensively covered the studies on lung and tracheal tissue engineering by bioprinting.

In this paper, the application of bioprinting technology to produce lungs and trachea is reviewed. First, a brief introduction on the structure of lung and tracheal tissues is provided to help better understand the criteria for 3D bioprinting techniques and bioinks. Then, we discuss the scaffold design criteria, important bioink properties, and applicable bioprinting techniques. Next, the studies attempting to engineer lungs and trachea using bioprinting are comprehensively reviewed, including the advances in alveolar mimicking and tracheal regeneration. Then, the remaining challenges and their possible solutions are highlighted. In the end, future directions are suggested to accelerate and facilitate the establishment of 3DP lungs and trachea for transplantation.

2. Criteria for bioprinting lung and tracheal constructs

In order for 3D bioprinting to be able to produce nature-like functional tissue constructs, it should meet certain criteria in both geometrical scaffold design and material characteristics. In this section, first, the structure of lungs is explained, followed by the criteria for lung and tracheal scaffold design by 3D bioprinting and available bioprinting techniques, with an evaluation of their capabilities and limitations regarding the mentioned criteria.

2.1. Structure and function of lungs and trachea

As the ultimate goal of lung tissue engineering by 3D bioprinting is to produce lung tissues mimicking the natural lungs, a proper understanding of lung structure and scaffold characteristics is needed to better understand and define criteria for 3D bioprinting. The lungs contain two main compartments: airway and vasculature. The airways are the core part of the pulmonary system, organized in a branched network (in a proximal-distal axis). There are 23 generations of airways, with 1.5 cm in diameter at the trachea to 0.5 mm at the respiratory bronchioles. Large airways are known as the conducting zone (i.e., no gas exchange occurs) of the lungs and start from the main bronchi to the terminal bronchioles. The smallest generations of airways are the respiratory bronchioles, leading into alveolar sacs and alveoli (Fig. 1D). Alveoli are small, interconnected spheres with an approximate diameter of 200 µm.

The necessary physiological functions of lungs are promoted by distinct local phenotypes resulting from region-specific epithelial differentiation that occurs along the proximal-distal axis. The epithelium of the tracheal and upper airway consists of columnar ciliated and mucous secretory cells, which contribute to capturing inhaled particles in mucus which are then expelled by cilia beating upwards. Club cells are cuboidal secretory cells that reside in the bronchioles and operate by secreted substances, including club cell secretory protein, to protect the

bronchiolar epithelium. The beginning of the distal respiratory zone is marked by terminal bronchioles transition into the alveoli. Alveoli contain two surfaces of air-containing (interior) and blood-bounded (exterior) [26]. The air-contacting surface is lined with epithelial cells, with the endothelial cells of the alveolar capillaries lying directly below. In the alveoli, alveolar type I cells facilitate gas exchange with their associated endothelial cells, and type II cells produce surfactants to maintain surface tension in the small volume of the alveolus [25,27].

Anatomically, the close connection of pulmonary vasculature with the airways along the proximal-distal axis is the main functional characteristic of the pulmonary vasculature. Smooth muscle-enrobed vasculature accompanies the upper airways, while the alveolar capillary bed, the densest in the whole body, consists of attenuated capillary endothelial cells with occluding junctions and no fenestrations, which confers tissue-specific fluid transport regulation [28,29].

The lung also exhibits special breathing-related mechanical properties. Lung compliance and elastance, impacting how much work is required to inhale air and reflecting how easily the lung recoils to its resting position after inflation, respectively, are conferred by collagenous and elastic fibers of the interstitial extracellular matrix (ECM) [30]. While decreased compliance (a stiffer lung) requires increased amount of work to inflate the alveoli, higher compliance results in difficulty exhaling [31,32].

On the other hand, the trachea has a simpler structure compared to the lungs. The trachea is a semi-flexible tube of 10–13 cm in length and 1.5–2 cm in diameter, which starts from the lower portion of the larynx and runs down behind the sternum. Then two smaller tubes called bronchi are branched from the trachea: the right main bronchus and the left main bronchus [33]. Also, the trachea is composed of 16–20 C-shaped cartilaginous rings anteriorly and a soft membranous trachealis muscle posteriorly. Moist, smooth tissue called mucosa lines the inside layer of the trachea. The trachea widens and lengthens slightly with each breath in, returning to its resting size with each breath out [34,35].

2.2. Scaffold design criteria and proper bioink properties

Meeting the criteria of scaffold design and fabrication is necessary to reach a suitable match between scaffolds and cells, which is a prerequisite to generate a functional tissue [36]. For example, to obtain functional 3DP lungs, scaffolds need to allow for appropriate gas exchange. Therefore, scaffolds are required to have viscoelastic behavior to allow proper ventilation of air through pressure change and provide extensive surface area and, most importantly, a sufficiently thin air-blood barrier to allow efficient gas exchange. To ensure that the lungs can transfer sufficient O_2 and CO_2, an alveolar surface area of ~130 m^2 is needed to obtain [37]. The air-blood barrier should simultaneously support the adhesion of a layer of cells and be able to sustain the fabrication process and the mild pressure during the use as failure to meet these criteria may result in blood leakage and eventually tissue dysfunction after implantation [38]. Regarding the trachea, the engineered/bioprinted scaffold needs to support new epithelialization, vascularization, and cartilage formation to reach the proper functionality and biomechanical properties after implantation. In addition, an ideal tracheal defect graft would degrade at the rate of the new tissue formation; faster degradation would result in 3DP trachea malacia, and prolonged degradation can promote foreign body inflammatory responses and then stenosis and scar formation [39].

The above-mentioned scaffold design criteria highlight the importance of utilizing bioinks with proper properties (Table 1). For example, the bioinks need to provide suitable mechanical strength and flexibility for the 3DP constructs to satisfy the viscoelastic behavior of the lungs, especially for the alveolar regions. Other mechanical properties are lung compliance and elastance. The total compliance of both lungs in an adult is about 200 ml/cm H_2O [40], and, on average, airways and parenchymal lungs are estimated to have elastic moduli in the range of 2.57–34.44 kPa and 0.64–5.13 kPa, respectively [41]. This range of elastic moduli can easily be achieved using soft hydrogels such as acellular collagen, Matrigel™, and alginate with a range of 0.5–12 kPa [42], 450 Pa [43], and 20 kPa [44], respectively. The other criteria that bioinks need to possess include biocompatibility, biodegradability, bioabsorbability, and printability. Bioinks should actively participate in lung and tracheal regeneration and also should not provoke any undesirable host responses after implantation. Furthermore, in specific cases like larger airways, the rate of degradation should be the same as the new tissue formation and accommodate tissue growth. This is important to allow the new ECM to be synthesized and organized by seeded cells so that the new ECM can support the structure of the tissue and be able to withstand mechanical loading caused by further cell seeding or surgical handling [45,46]. Hence, the use of smart or 4D materials, whose properties change by time or some external stimuli, is beneficial. Also, the degraded materials should be non-toxic and safely absorbed by the body. Bioinks also need to be polymerized using different gelation methods. This would make it possible to apply different types of bioprinting methods if needed. All of these characteristics help to approach biomimicry and exact imitation of the functional properties of the lungs and trachea.

Table 1
Summary of the main requirements of lung and tracheal 3D bioprinting that bioprinters and bioinks need to satisfy.

	Requirements and Their Roles/Definitions
Bioprinters	*Nozzle Size*. The smaller the nozzle size, the higher the resolution. However, the effect of high shear stress on the cells should be considered in nozzle-based bioprinters
	Print Speed. Printing with optimum speed so that bioinks and cells are completely preserved during printing
	Multi Nozzles Supporting. The ability to support different types of nozzles to optimally print different parts of the tree structure of the lungs (supporting the size and resolution of trachea to alveoli)
	Multi Cells and Bioinks Supporting. The ability to print multiple cell types simultaneously, especially the endothelial-epithelial structure of the air-blood barrier; and support different bioinks at the same time
Bioinks	*Biomimicry*. Accurate imitation of the functional specific properties of the trachea and lungs
	Biocompatibility. Having no or minimum undesirable host responses, in addition to active participation in lung and tracheal regeneration
	Biodegradability and Bioabsorbability. The rate of degradation should be the same as the new tissue formation rate (e.g., using smart or 4D materials), and the degraded materials should be non-toxic and absorbed by the body
	Structural Properties. The material should provide the printed construct with suitable mechanical strength and also satisfy the host tissue mechanical requirements (from flexible alveoli to rigid bronchi)
	Printability. The ability to be printed for specific processes by the bioprinters (proper viscosity, gelation methods, shear-thinning) and ideally applied as a universal bioink for the whole of the construct

2.3. Bioprinting techniques: function and applicability to meet the criteria

Among various techniques of nozzle-based and nozzle-free printing, four bioprinting types are the most common in tissue engineering: the inkjet, laser-assisted, extrusion, and stereolithography bioprinting, each of which have their specific advantages and limitations. These bioprinters have been reviewed in detail in previous studies [47,48]. However, the following briefly describes the function, advantages, and disadvantages of these 3D bioprinters, followed by the criteria that bioprinters need to satisfy for a successful and reliable lung and tracheal bioprinting. A comprehensive comparison of the common bioprinting techniques is provided in Table 2 as well.

In inkjet bioprinters, the bioink is stored in a cartridge, and the cartridge is connected to a printer head. As shown in Fig. 1E, during printing, the printer heads are deformed by an actuator (e.g., thermal or piezoelectric actuator) and pressed to generate droplets. For laser-assisted bioprinting, similar to inkjet printing, the additive unit is drop. A laser-assisted printer comprises a pulsed laser beam, a ribbon structure containing a donor transport support that is covered with a laser-energy-absorbing layer (on top) and a bioink layer (on bottom), and a receiving

Table 2
Main properties of 3D bioprinters applicable for lung and tracheal tissue engineering.

	Bioprinter Type				References
	Inkjet	Laser-assisted	Extrusion	Stereolithography	
Figure Address	Fig. 1E	Fig. 1F	Fig. 1G	Fig. 1H	–
Gelation Methods	Chemical Photo-crosslinking	Chemical Photo-crosslinking	Chemical Photo-crosslinking Sheer thinning Temperature	Photo-crosslinking	[133–136]
Additive Unit	Drop	Drop	Strain	Cured bioink voxel	[137]
Actuation Method	Piezoelectric pulse Thermal induced pulse Acoustic actuator Pneumatic actuator	Laser-induced pulse	Pneumatic pressure Mechanical pressure (piston or screw) Electromagnetic driver	Laser-based curing UV and visible light projection curing	[47,136]
Cell Viability	>85%	>95%	40–95%	>85%	[138–140]
Cell Density (cells/ml)	Low $< 10^6$	Medium $< 10^8$	High cell spheroids	Medium $< 10^8$	[48]
Bioink Viscosity (mPa/s)	Low 3.5–12	Medium 1–300	High 30–6 × 10^7	Medium <5000	[141–144]
Resolution	High 50 μm wide	High 10 μm wide	Moderate 100 μm wide	High 50 μm wide	[51,145–149]
Vertical Printing Quality	Poor	Medium	Good	Good	[147]
Print Speed	Fast up to 10,000 drop/s	Medium 200–1600 mm/s	Slow 10–50 μm/s	Fast	[48,150]
Printer Cost	Low	High	Moderate	Low	[151,152]
Commercial	✓	×	✓	✓	[48]
Overview of Main Advantages and Disadvantages	✓ ability to print low viscosity biomaterials ✓ fast fabrication speed ✓ low cost ✓ high resolution × inherent inability to provide a continuous flow × poor functionality for vertical structures × low cell densities	✓ nozzle-free technique ✓ high printing resolution ✓ deposition of biomaterials in solid or liquid phase × low diversity of bioink for ribbon preparation × high cost × thermal damage due to nanosecond/femtosecond laser irritation	✓ allowing high cell density ✓user-friendly (simplicity) ✓ capable of printing various biomaterials × shear stress may affect the cells × applicable only for viscous liquids	✓ nozzle-free technique ✓ high print speed ✓ printing time is independent of the complexity ✓ high accuracy and cell viability × applicable only for photo-crosslinking bioinks × multicellular structures are challenging × damage to cells during photocuring or due to UV light toxicity	[47–51,137, 147,153–157]

substrate facing the ribbon (Fig. 1F). The laser pulse vaporizes a portion of the donor layer, causing the bioink to fall. The falling bioink droplet is then collected on the receiving substrate and subsequently crosslinked. Extrusion bioprinters are a modification of inkjet printers; the bioink is stored in a cartridge, and the cartridge is connected to a printer head. As shown in Fig. 1G, extrusion printing uses a pneumatic or mechanical pressure to dispense viscous bioinks that inkjet printers cannot deposit. Using a continuous force, extrusion bioprinters print uninterrupted cylindrical lines rather than a single bioink droplet at a time. Stereolithography bioprinters, like laser-assisted printers, use light to selectively polymerize a bioink in a layer-by-layer process. These printers use laser-based curing or ultraviolet (UV) and visible light projection to cure bioinks plane-by-plane (Fig. 1H).

Despite the significant developments in speed, precision, and resolution of printing, each of the above-mentioned bioprinters has its own limitations. Inkjet printers, for example, possess high printing speed and are obtainable at a low cost, but they cannot print quality and functional vertical structures. Laser-assisted printers can achieve high resolutions but cannot quickly print voluminous scaffolds. On the contrary, extrusion printers can print quickly but are limited to a resolution of approximately 100 μm. Stereolithography printers provide the high resolution required for printing alveolar sacs and produce voluminous constructs with complex geometry at high speed; however, their applications are limited only for photo-crosslinking bioinks [49–52].

Regardless of what bioprinter type is used, there are some criteria that bioprinters need to have to successfully produce reliable lung and tracheal constructs (Table 1). Bioprinters need to be able to support multi nozzles of different types at once to print different parts of the lungs; for example, a nozzle using a bioprinting technique is needed to support the size and structure of the trachea, and another nozzle supporting another bioprinting type is required to print alveoli in a micro-nano resolution. Another requirement is the ability to print multiple cell types simultaneously to deposit the cells in their specific region during the printing. For example, in printing the air-blood barrier, producing a functional epithelium facing the alveolar lumen and an endothelium facing the capillary lumen is critical. The other important criterion is the print speed. Optimal print speed is crucial to preserve the bioinks and cells during printing, as prolonged printing processes result in reduced cell viability [53]. Increasing the speed of the nozzle head movement, decreasing the distance of the tip from the surface, and increasing the material flow rate by using bioinks with lower viscosities are approaches to speed up the extrusion bioprinting, for example. Furthermore, in nozzle-based bioprinters like inkjet and extrusion printers, the nozzle size is important. Although smaller sizes of nozzles and tips result in higher resolutions, in extrusion printers, encapsulated cells may suffer from large mechanical stresses, which leads to reduced cell viability [54].

All in all, regarding bioprinting of lung parenchyma tissue, while other types of bioprinting lack the desired resolution or vertical printing quality required for high constructs, stereolithography provides the high resolution required for printing alveolar sacs and produces voluminous constructs with complex geometry in a short time. Also, considering the tracheal structure, geometry, and biophysical properties, extrusion bioprinters are a better option as they support high cell density, high bioink viscosity, and various biomaterials printing.

3. Advances in lung and tracheal tissue engineering using 3D bioprinting

3D bioprinting has been utilized as one of the attractive and reliable methods for engineering lung and tracheal tissues, with the ultimate goal of producing transplantable grafts. This section first discusses the advancements in lung bioprinting and then reviews the studies on

producing bioprinted tracheal grafts, highlighting the most used polymers, followed by a review on the non-polymer based approach adopted to produce 3D bioprinted tracheas.

3.1. Bioprinting of the lungs: mimicking the alveolar function

The primary function of the lungs is the process of gas exchange. Alveoli are a part of the lungs in which the gas exchange occurs between blood and air through a thin membrane called air-blood barrier [55]. 3D bioprinting of alveoli-mimicking structures is challenging mainly due to the complexity and size scale of the alveoli (~200 μm) [56] and air-blood barrier (0.62 ± 0.04 μm) [57]. The following reviews the two pioneer studies investigating the 3DP alveoli-like structures (Table 3).

Horvath et al., in 2015 printed a gelatinous protein mixture (Matrigel™) with endothelial and epithelial cells and reached thinner and more homogeneous cell layers compared to manual methods, which is necessary for an optimal air-blood barrier (Fig. 2A and B). Although the obtained barrier was not suitable enough to be translated into an implantable engineered tissue, this study was a major step towards validating printed lung tissues and provided great potential for *in vitro* toxicology and pharmaceutical assessments for basic lung studies [58]. Also, Grigoryan et al., in 2019 printed a complex geometry using PolyEthylene Glycol DiAcrylate and created a distal lung model with vascular and airway spaces. They demonstrated oxygen transportation by measuring the oxygen level of the human red blood cells during tidal air ventilation (Fig. 2C and D). The airway space in this study was in millimeter dimensions and had no cell components; therefore, it needs to satisfy the micro size scale of the real alveolar structures to become clinically translatable. However, this study was huge progress towards producing a real-like lung tissue [23].

3.2. Bioprinting of the trachea: tracheal defect grafts

The trachea is a connection between the larynx and bronchi, which regulates breathing [59]. To treat acute tracheal disorders, conventional methods such as the use of artificial implants, allografts, and autogenous grafts have been inefficient in terms of functionality in long terms [60]. Therefore, 3D bioprinting technique has been employed to produce engineered tracheal grafts as an alternative approach. Using this approach, the majority of studies utilized a combination of synthetic and natural polymers with different biodegradability rates for specific cases (Table 4). Organoid printing technique was also applied to produce 3DP tracheal constructs without the use of polymers. The results show that mesenchymal stem/stromal cells (MSCs) are an ideal-like cell source for 3DP tracheal grafts as they facilitate tissue integration after implantation. Also, applying computer-aided design and simulation technologies resulted in personalized custom-designed 3DP tracheal grafts (Fig. 3A), suggesting that similar approaches can be used in lung tissue bioprinting.

3.2.1. Polymer-based studies

The usual technique for polymer-based 3D bioprinting of tracheal grafts is to combine synthetic polymers as supporting materials with natural polymers seeded with cells like chondrocytes or epithelial cells. Examples for synthetic polymers are polycaprolactone (PCL) and polylactic acid (PLA), while biological hydrogels like collagen, fibrin, alginate, or even decellularized extracellular matrix (dECM) are used as natural polymers.

PCL, as the most used synthetic polymer, is a biocompatible polymer that is also biodegradable and bioabsorbable [61]. In addition, PCL takes up to three years to degrade [62], making it a suitable material to be used in temporary cases where the new tissue formation rate is relatively low. Due to these characteristics, PCL has received great attention in producing tracheal defect grafts (Fig. 3B) [19–22,60,63–68]. While implanting of PCL tracheal grafts with no seeded cells resulted in minimal tissue integration in sheep [22], adding a hydrogel of alginate plus collagen type I seeded with chondrocytes to PCL scaffolds improved the fibrous tissue formation after implantation into rabbits [65]. The benefits of using the matrix and cells together in tracheal bioprinting were exemplified in another study using a five-layer PCL graft with alginate seeded with epithelial cells and chondrocytes. While out of 15 rabbits received these grafts, 13 survived, half the rabbits which received PCL-only scaffolds with no cells died from respiratory symptoms (3 out of 6). In addition, utilizing epithelial cells resulted in effective respiratory epithelium regeneration [20].

PLA, polylactide caprolactone (PLCL), polycarbonate (PC), and polyurethane (PU) are other polymers that have been used for producing 3DP tracheal grafts. PLA degradation rate varies between 12 and 16 months, depending on its different forms. PLCL is a copolymer of PLA and PCL. Depending on the composition ratio, it degrades between 12 and 24 months and has appropriate mechanical properties for tracheal defect grafts [62]. Implantation of a tracheal graft made from PLA and collagen type I seeded with chondrocytes resulted in a well-mucosalized tracheal lumen and new cartilage formation [69]. Similarly, using PLCL with chondrocytes in gelatin directed the tracheal cartilage formation *in vivo* when implanted into the dorsal subcutaneous spaces of nude mice. The construct also showed an appropriate mechanical behavior similar to the native trachea [70]. Furthermore, porous or solid PC rings were tested *in vitro* to approximate the biomechanical properties of native sheep trachea. The most appropriate constructs then underwent vacuum seeding with ovine bone marrow-derived mononuclear cells. It was shown that while the porous rings were most biomimetic, cell seeding into the solid rings was more efficient as evidenced by fluorometric DNA assay [71]. Furthermore, to avoid the potential mismatch between the scaffold degradation and neo-tissue formation, non-biodegradable PU was used to fabricate 3DP tracheal grafts. After implantation of cell-free grafts in rabbits, re-epithelialization and ingrowth of connective tissue with microvasculature were seen. However, further verifications are needed to prove that the non-biodegradable PU has the adequate qualification to provide the necessary biomechanical function for the host trachea with no need for new cartilage regeneration for long terms [72].

A large number of studies on 3DP tracheal grafts with polymers have utilized MSCs in order to mature the construct. MSCs are pluripotent stem cells that, under appropriate stimulations, are able to differentiate to various cells, including osteoblasts, chondrocytes, adipocytes,

Table 3
Studies applying 3D bioprinting to mimic the alveolar function.

Scaffold/ Material	Cell Sources	Key Points	Printing method	Figure Address	Reference, Year
Matrigel™	Endothelial cells (EA.hy926), Epithelial cells (A549)	✓ creation of thinner and more homogeneous cell layers compared to manual method; great potential for *in vitro* toxicology and pharmaceutical assessment × difficult translation to an implantable engineered tissue	ECM by contact dispensing and cells by jetting using BioFactory™	Fig. 2A and B	[58]
PEGDA	–	✓ complex geometry of distal lung model with vascular and airway spaces × the dimensions were in millimeters, and the structure had no cell components	Stereolithography	Fig. 2C and D	[23]

Matrigel™: a gelatinous protein mixture. **PEGDA**: PolyEthylene Glycol DiAcrylate.

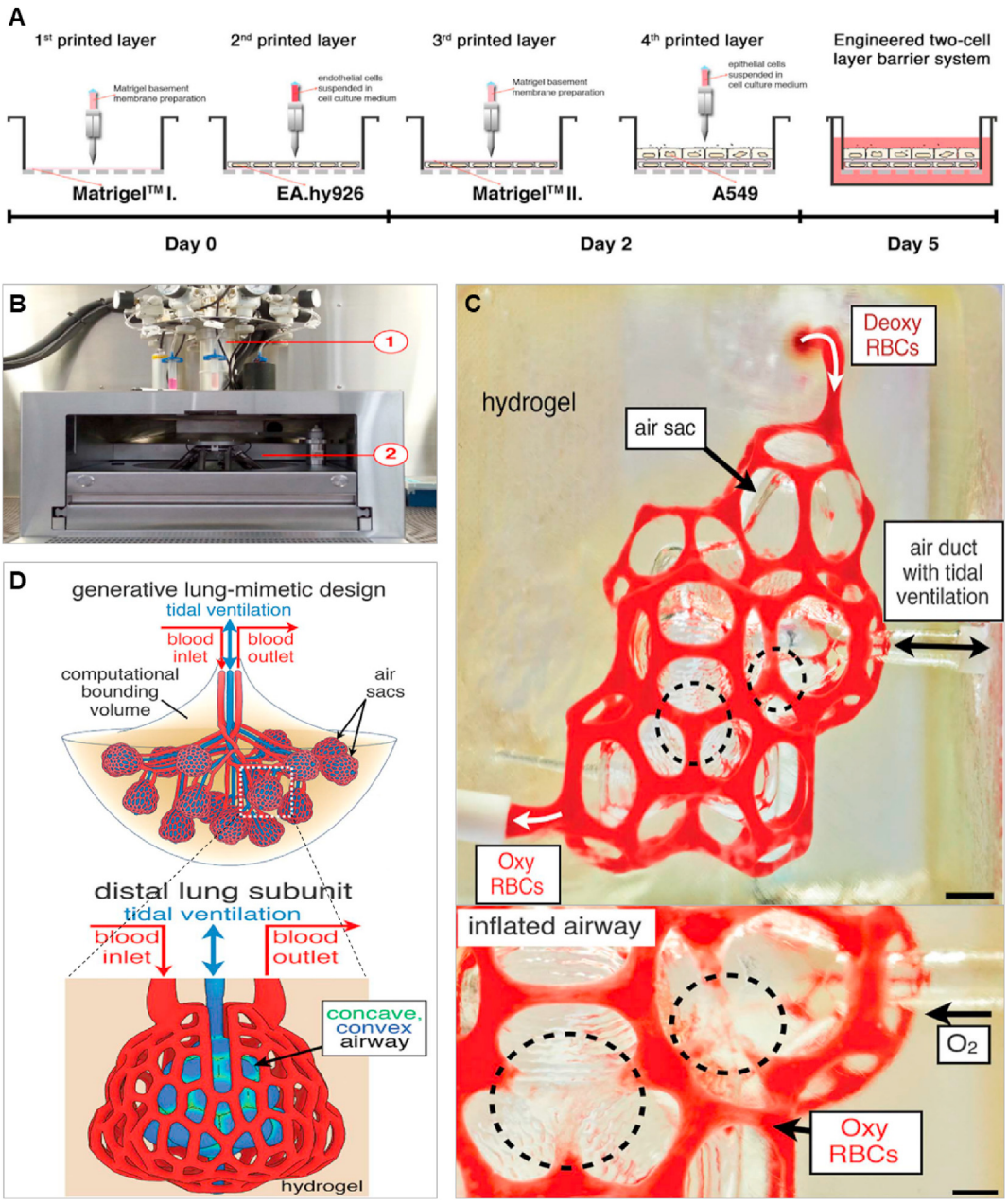

Fig. 2. Alveolar function mimicking using 3D bioprinting. (**A–B**) Schematic illustration of the cell patterning timeline process and the bioprinting system. **(A)** Schematic of the timeline for bioprinting a two cell-layer barrier system. EA. hy926 endothelial cells and A549 epithelial cells were printed on day 0 and day 2, respectively. On day 5, the 3D organization, viability, and proliferation of the cells, as well as barrier quality, were assessed. **(B)** The process unit of a commercial bioprinter comprising the tool changer (1) with three workstations equipped with print heads and the building cell area with the building platform (2), reproduced/adapted with permission from Ref. [58]. **(C–D)** Hydrogels with vascularized alveolar model topologies during tidal ventilation and oxygenation. **(C)** (Top) Photograph of a printed alveolar model during red blood cells (RBC) perfusion and air sac ventilation with O_2 (scale bar, 1 mm). (Bottom) Concave regions of the airway (dashed black circles) squeezed adjacent blood vessels and caused RBC clearance when airway inflation with oxygen occurred (scale bar, 500 μm). **(D)** (Top) A generative lung-mimetic design based on growth of the airway, offset growth of opposing inlet and outlet vascular networks, and population of branch tips with a distal lung subunit. (Bottom) The distal lung subunit consists of a concave and convex airway ensheathed in the vasculature, reproduced/adapted with permission from Ref. [23]. (For interpretation of the references to colour in this figure legend, the reader is referred to the Web version of this article.)

endothelial cells, nerve cells, heartmyocytes, hepatocytes, and pancreatic cells [73]. It has been proved that the existence of the MSCs on the tracheal scaffolds improves the new tissue formation after implantation. For example, when used in a graft formed of PCL and fibrin, successful integration of the implanted graft with the adjacent trachea was observed, and the shape and function of the host trachea were restored [63]. In addition, the use of human turbinate MSC sheets with a PCL-collagen graft accelerated tracheal epithelial regeneration by producing a mature and highly-ciliated epithelium on the surface of the 3DP grafts implanted in rabbits [64]. In another study, MSCs were first cultured in chondrogenic media and then seeded on alginate alongside epithelial cells. This cell combination helped the PCL-alginate graft to form the neo-cartilage, neo-epithelialization, and neo-vascularization *in vivo*, which are the necessary factors to reach an ideal-like tracheal graft [21].

3.2.2. *Organoid printing (non-polymer based)*

Relying heavily on polymers as supporting structures for cells in tracheal bioprinting may cause some limitations, such as design inflexibility and cytocompatibility issues [74]. Therefore, support-free

Table 4
Studies investigating 3D-printed (3DP) tracheal grafts.

Polymer Type	Scaffold/Material	Cell Sources	Species	Key Points	Figure Address	Reference, Year
Biodegradable	PCL + fibrin	MSCs	Rabbit	✓ successful integration of the implanted 3DP tracheal grafts with the adjacent trachea × qualitative and not quantitative analyses	–	[63]
	PCL + collagen	hTMSCs sheets	Rabbit	✓ accelerated tracheal epithelial regeneration × unclear role of hTMSCs whether as part of the columnar epithelium or as an accelerator of native cell migration and maturation	–	[64]
	PCL + decellularized bovine dermal ECM	MSCs (only *in vitro* purposes)	Pig	✓ implantation in a large animal model × granulation at the graft interface because of the immune response to the rapid resorption of ECM by the host's cells	Fig. 3B	[19]
	PCL + alginate	Epithelial cells, MSCs	Rabbit	✓ neo-epithelialization and neo-vascularization *in vivo* × neo-cartilage formation only in groups cultured in chondrogenic media	–	[21]
	PCL + alginate	Epithelial cells, Chondrocytes	Rabbit	✓ effective respiratory epithelium regeneration × unsuccessful cartilage regeneration	Fig. 3D–F	[20]
	PCL + alginate/ collagen I	Chondrocytes	Rabbit	✓ formation of a thin layer of fibrous tissue around the PCL scaffold × inadequate or immature cartilage formation with inflammation for areas without membranous coverage	–	[65]
	PCL (3DPand electrospun)	–	Sheep	✓ easy to implant, therefore, suitable for emergency surgery × minimal tissue integration into the patch	–	[22]
	PCL + collagen	–	Rabbit	✓ off-the-shelf, therefore, suitable for urgent implantation × long-term investigation needed to evaluate the performance of the non-biodegradable silicon rings used as an alternative to tracheal cartilages	–	[66]
	PCL	Chondrocytes	Goat	✓ 3DP tracheas resulted in higher post-operative survival times compared with autologous trachea grafts × tracheal narrowing after implantation	–	[60]
	PCL	MSCs (only *in vitro* purposes)	–	✓ significant increase in maximum stress and elastic modulus for 3DP tracheal grafts compared with native tracheal patch × no *in vivo* implantation	–	[67]
	PCL + collagen + hyaluronic acid	MSCs (only *in vitro* purposes)	–	✓ the first study of its kind to fabricate bioprinted tracheal constructs with separate cartilage and smooth muscle regions × no *in vivo* implantation	–	[68]
	PLA + collagen I	Chondrocytes	Rabbit	✓ well-mucosalized tracheal lumen with no evidence of scarring or granulation tissue × lack of a control group in the *in vivo* segment	–	[69]
	PLCL + gelatin (in a 3DPsacrificial mold)	Chondrocytes	Mouse	✓ appropriate mechanical behavior similar to the native trachea and tracheal cartilage formation *in vivo* × potential functional challenges because of less flexibility of collagen when it replaces the PCL/gelatin scaffold after degradation	Fig. 3A	[70]
	PC + (electrospun PET + PU)	Ovine bone marrow-derived mononuclear cells	–	✓ approximation of the biomechanical properties of the native ovine trachea × no *in vivo* or *ex vivo* testing	–	[71]
Non-Biodegradable	PU	–	Rabbit	✓ re-epithelialization and ingrowth of connective tissue with microvasculature after implantation × verification needed to prove whether the non-biodegradable PU may compensate for the native trachea's biomechanical function with no need for new cartilage regeneration	–	[72]
Non-Polymer Based	Organoid printing	Chondrocytes, Endothelial cells, MSCs	Rat	✓ histologically observation of chondrogenesis and vasculogenesis × verification needed to prove whether the microvessels were host or donor-derived	–	[74]
	Organoid printing	Chondrocytes, HUVECs, MSCs, Fibroblasts	Rat	✓ viability of the small-diameter trachea-like tubes *in vivo* and proliferation of tracheal epithelium and capillaries × lower strength of the trachea-like tubes compared to that of the native trachea	Fig. 3C	[75]

ECM: ExtraCellular Matrix. **hTMSCs**: Human Turbinate Mesenchymal Stromal Cells. **HUVECs**: Human Umbilical Vein Endothelial Cells. **MSCs**: Mesenchymal Stem/ Stromal Cells. **PC**: PolyCarbonate. **PCL**: PolyCaproLactone. **PET**: PolyEthylene Terephthalate. **PLA**: PolyLactic Acid. **PLCL**: Poly Lactide CaproLactone. **PU**: PolyUrethane.

approaches can be a promising solution to overcome the mentioned issues. A method of support-free 3D bioprinting is called organoid printing (Fig. 3C). The first feasibility assessment of this method to produce tracheal grafts was reported by Taniguchi et al., in 2018. In this study, chondrocytes, endothelial cells, and MSCs were used to form multicellular spheroids. A removable needle array was then used to organize these spheroids into a tracheal structure. After the needles were removed, a silicone stent was placed in the lumen to prevent lumen compaction and to make it strong enough for transplantation. The 3DP tracheal graft was matured in a bioreactor and then implanted into rats. Histology examinations confirmed the chondrogenesis and vasculogenesis [74]. Also, using fibroblasts alongside other cells resulted in a cartilaginous-fibrous tube more resembling the structure of the native trachea. The viability of the trachea-like tubes *in vivo* and the proliferation of tracheal epithelium and capillaries were confirmed after implantation into rats [75].

All in all, among various printing techniques, stereolithography and extrusion methods were utilized for 3D bioprinting of alveoli-mimicking structures, while for producing bioprinted tracheas, extrusion and

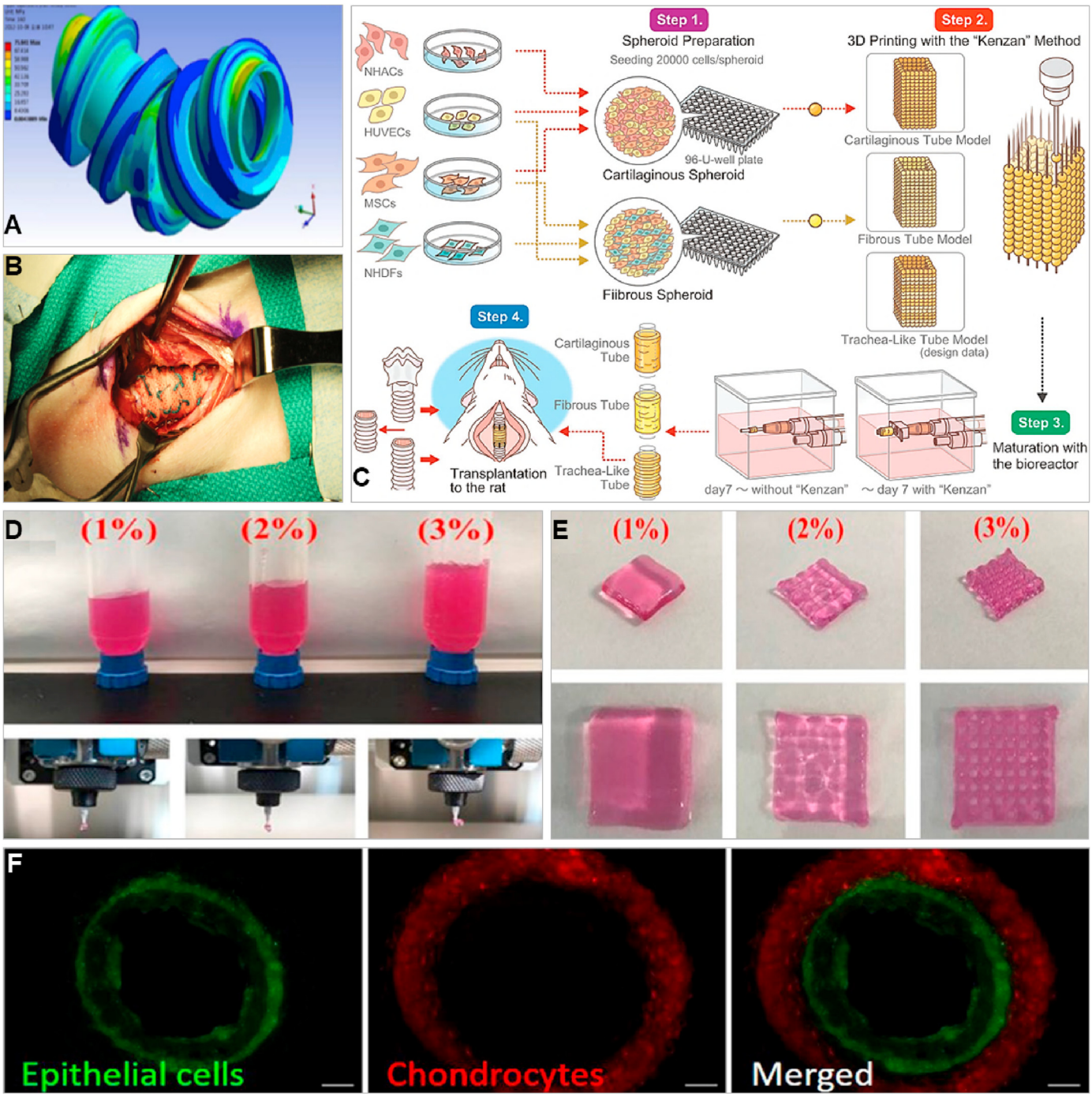

Fig. 3. Simulation, production process, and assessments of 3D-printed (3DP) tracheal grafts. (**A**) Simulation of luminal deformation and stress distribution for the whole trachea, reproduced/adapted with permission from Ref. [70]. **(B)** A size-matched 3DP PCL-ECM graft implanted to a pig, reproduced/adapted with permission from Ref. [19]. **(C)** Schematic of organoid printing including step 1: spheroid preparation with different cell types, step 2: 3D bioprinting of tubes, step 3: maturation with the proper medium flow in a bioreactor, and step 4: transplantation to a rat, reproduced/adapted with permission from Ref. [75]. **(D–F)** 3DP cell-laden alginate as the natural polymer in a tracheal construct. **(D)** Alginate hydrogel with three different concentrations being extruded at a 300 μm nozzle. **(E)** Optical image of 3DP cubic alginate ($16 \times 16 \times 2$ mm^3). The higher concentration of alginate hydrogel (3%) provided more precise and porous constructs. **(F)** Fluorescent microscopic images using green dye for the epithelial cells (Left) and red dye for chondrocytes (Middle); merged image (Right) revealed that the two hydrogel layers were completely separated as a PCL layer was printed between them, scale bar: 100 μm, reproduced/adapted with permission from Ref. [20]. (For interpretation of the references to colour in this figure legend, the reader is referred to the Web version of this article.)

stereolithography bioprinting were adopted as well as organoid printing. Organoid printing has recently been developed for tracheal graft production for small rodents. While it has satisfied the criteria required for 3DP tracheas by replacing the epithelium and capillaries lost in rat tracheas, further experiments in large animal models are required to move towards clinical application. On the contrary, the extrusion method has been widely utilized for tracheal bioprinting even for large-sized constructs but is not qualified enough to print delicate alveolar structures with high resolutions. In addition, some studies have utilized stereolithography for tracheal bioprinting. Considering the fact that stereolithography has shown to be promising in producing constructs that mimic the alveolar structure and function, and that it could be used to

simultaneously print the lung parenchyma and tracheal tissues, it would be expected that this method would see more progress.

4. Challenges and potential solutions

3D bioprinting has many advantages in comparison to traditional methods, including co-printing of materials and cells in a multi-layered form and printing complex patterns, which makes 3D bioprinting beneficial for producing hollow structures like lung constructs. However, there remain challenges in achieving functional whole lungs and trachea. The need for vascularization closely adjacent to the alveoli and complex patterning of the heterocellular portions is among the main challenges, which requires high resolutions to print such fine structures; however, high-resolution printing is often associated with cell-damaging processes with high shear stress in nozzle-based bioprinting methods, highlighting the advantage of the nozzle-free printing techniques such as stereolithography [76]. There is also a need for a rapid printer that can print a combination of voluminous materials with one or more cell types without damage to the cells in a high resolution at micro to nano scales to produce real-like alveolar structures to become clinically translatable. The following describes the specific challenges and their potential solutions regarding engineering lungs and trachea via bioprinting.

4.1. The lungs

Lung tissue has a complex 3D structure and requires thin boundaries and interconnected pores for efficient gas exchange [77]. Bioprinting such structures is faced with limitations. First, as bioinks are usually soft and printed in a vertical structure for lung fabrication, improved structural support techniques to prevent the lung from collapsing under its own weight during printing are required. The freeform reversible embedding of suspended hydrogels (FRESH) method has proved to be a potential approach for printing complex architectures out of soft materials that cannot be printed in a vertical structure in the air (Fig. 4A).

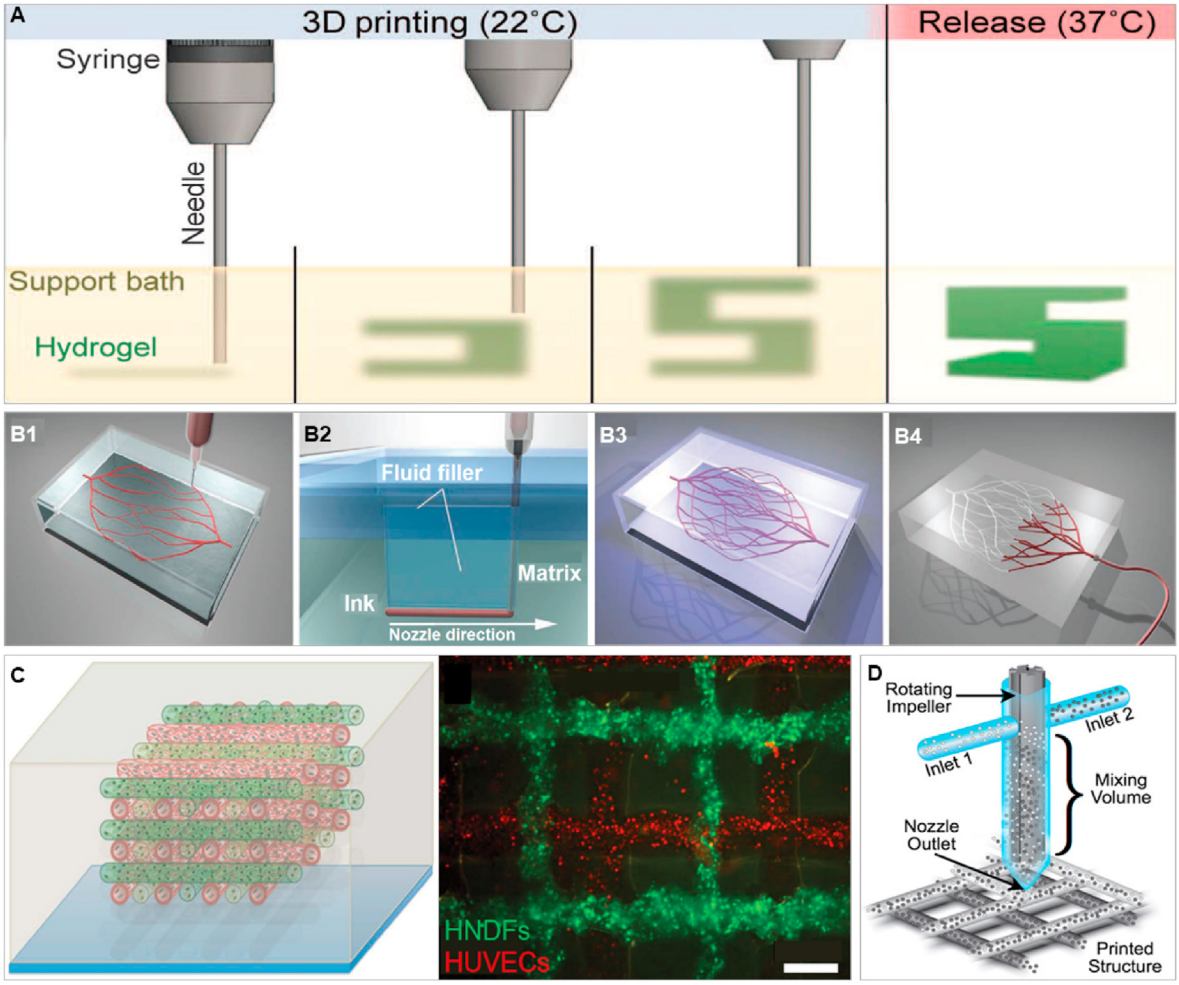

Fig. 4. Approaches to support printing of soft bioinks (A), hierarchical vascularization (B1–B4, C), and graded printing (D) to facilitate lung and tracheal 3D bioprinting. **(A)** 3D bioprinting of soft hydrogels by Freeform Reversible Embedding of Suspended Hydrogels (FRESH) method. The FRESH method uses gelatin as a support bath (yellow) to provide temporary support for the hydrogel (green). After the hydrogels are printed, gelatin is heated to 37 °C to release the printed construct, reproduced/adapted with permission from Ref. [79]. **(B1–B4)** Omnidirectional 3D printing of microvascular networks within a hydrogel reservoir. Deposition of a fugitive ink into a physical gel reservoir **(B1)** allows hierarchical and branching networks to be patterned. Voids induced by nozzle translation are filled with liquid that migrates from the fluid-capping layer **(B2)**. Subsequent photopolymerization of the reservoir yields a chemically crosslinked hydrogel matrix **(B3)**. The ink is liquefied and removed under a modest vacuum to expose the microvascular channels **(B4)**, reproduced/adapted with permission from Ref. [80]. **(C)** A 3D bioprinting approach in which vasculature, cells, and ECM are co-printed to yield engineered, vascularized, and heterogeneous cell-laden tissue constructs (left: schematic, right: fluorescence); red and green filaments correspond to channels lined with HUVECs- and HNDFs-laden bioink, respectively. Scale bars, 300 μm, reproduced/adapted with permission from Refs. [82]. **(D)** Tunable graded 3D bioprinting of biomaterials with different viscosities and biochemical properties using a mixing nozzle, reproduced/adapted with permission from Ref. [83]. (For interpretation of the references to colour in this figure legend, the reader is referred to the Web version of this article.)

Using this technique, an embryonic chick heart with alginate and a perfusable vasculature geometry with collagen were printed while gelatin microparticles were used as the support bath. The gelatin microparticles provided the Bingham plastic properties to facilitate the printing, i.e., solid at low shear stresses and viscous at high shear stresses [78,79]. This technique can print large scaffolds on a scale of millimeters to centimeters with microscale resolution (~200 μm). Such a resolution scale is suitable for printing the trachea and other larger airways, but it is far from the resolution required for structures such as alveoli (Fig. 1D). However, by applying higher-precision printers, smaller-diameter needles, and gelatin slurries with smaller particle diameter, higher resolutions are achievable.

Another challenge in lung 3D bioprinting is the hierarchical 3D architecture of the multiscale vascular network that branches with airway generations. A potential approach is omnidirectional printing (ODP) of microvascular networks within a hydrogel reservoir by direct ink writing [80]. In ODP, fugitive bioinks are printed within a photocurable gel reservoir that physically supports the patterned features. The fugitive bioink can then be liquefied and removed to expose the microvascular channels within the matrix (Fig. 4B1-B4). Another approach is co-printing of vasculature, cells, and ECM to yield engineered, vascularized, and heterogeneous cell-laden tissue constructs. Using this approach, vasculature lined with endothelial cells and biomaterials encapsulating MSCs and fibroblasts within a customized ECM were co-printed (Fig. 4C) [81,82].

Furthermore, printing bioinks with graded properties is another critical aspect of lung bioprinting. This is necessary when bioinks with varying viscosities and biochemical properties are printed in specific regions of the lungs, ranging from alveolar portions with a flexible structure to bronchioles and bronchi with more rigid geometry. A promising approach is the use of mixing nozzles that can dispense materials, with tunable gradients of differing material properties (Fig. 4D) [83].

4.2. The trachea

Despite all the progress, there remain two significant challenges in tracheal tissue bioprinting. First, further improvements are needed to promote the neo-cartilage formation, neo-epithelialization, and neovascularization *in vivo* to reach an ideal tracheal graft. Second, qualified biomechanical properties tolerating against motion forces with proper rate of degradation need to be considered when designing and printing tracheal constructs. To deal with the first challenge, although the use of cell lines like chondrocytes, epithelial, and endothelial cells is necessary and beneficial, the use of stem cells like MSCs is recommended as it facilitated tissue integration and maturation after implantation [63,64]. Meeting the second criterion requires applying a combination of degradable synthetic polymers like PCL and natural polymers like dECM as it promoted the construct's mechanical properties and tissue integration before and after transplantation, respectively [19,21]. Also, to improve the biological integrity and biomechanical function after transplantation, porous structures are promising [64,66,70], as they increase the potential of cell infiltration and ingrowth, leading to increased tissue integrity.

5. Future directions

Considering the complexity of lung and tracheal tissue bioprinting, the following suggests a universal bioink approach with an emphasis on dECM and applying human pluripotent stem cells to improve the structural and functional properties of 3DP lungs and trachea. Next, a potential approach regarding bioprinters is suggested by leveraging stereolithography technology. Also, to mature the constructs and perform simulation of *in vivo* conditions before transplantation, monitoring bioreactors are presented.

5.1. A universal bioink

To support both the region-specific lung cells and to satisfy the biomechanical properties of the hierarchical structure of lungs when bioprinting, bioinks with different biochemical and mechanical properties might be needed. Natural proteins such as collagen, elastin, fibronectin, and laminin have been widely used as a biomaterial for tissue engineering and regenerative medicine purposes as such proteins are highly biocompatible and naturally promote cell adhesion, proliferation, and differentiation. However, hydrogels formed by neat fibers of such proteins are not suitable enough to be used as a bioink due to the inherent weak mechanical properties of these proteins, especially for stereolithography bioprinting method, which is getting much attention in lung bioprinting.

One promising option would be developing a universal bioink that would both support different cells' proliferation and differentiation and possess controllable mechanical properties, applicable for stereolithography or any other type of bioprinting. Such a universal bioink would be achievable whether by modification of natural proteins or using hybrid materials composed of ECM proteins and biocompatible synthetic polymers [46]. For example, a research group modified type-I collagen to collagen methacrylamide, as a fibril-forming bio-ink, making it suitable for stereolithography bioprinting [84]. Also, gelatin methacrylate (GelMA), a photopolymerizable hydrogel comprised of modified natural ECM components, was demonstrated to be an inexpensive, cell-responsive hydrogel platform for creating cell-laden tissues, while possessing high pattern fidelity and a controllable biodegradability [85]. When resins of fish and porcine-derived GelMA were formulated in formamide using GelMA alone or mixed with star-shaped PCL methacrylate (PCL-MA) to obtain a GelMA-based resin for high-resolution tissue scaffolds, the PCL-MA in the hybrid resins promoted the 3D printing fidelity compared with the neat GelMA resins. The same process was applied for native organ-derived materials by replacing GelMA in the hybrid resin with solubilized, methacryloyl-functionalized decellularized liver ECM (dECM-MA). Multi-layer dECM/PCL-MA hydrogels were printed by stereolithography [86]. In another study, a printable resin composed of 10% GelMA with various concentrations of polyethylene glycol diacrylate (PEGDA) was made to bioprint cartilage constructs using a tabletop stereolithography-based 3D bioprinter [87]. Also, two different concentrations of GelMA macromer (7.5 and 12.5%) were used for visible light-based stereolithography bioprinting of corneal stroma, showing that scaffolds with 12.5% GelMA concentration were closer to the native corneal stroma tissue in terms of water content and optical transmittance [88].

Overall, biomaterials obtained from modified natural proteins or hybrid materials (e.g., a combination of ECM proteins and biocompatible synthetic polymers) could be considered as a universal bioink as they support various cell types and are compatible with different bioprinting platforms, especially stereolithography. Because whole or most of the content of such substances is comprised of natural materials, these bioinks are native-like and recognizable to the human body. Also, such biomaterials have the appropriate mechanical and biochemical properties to both support straightforward printing procedures and mature the construct by providing the required post-printing mechanical properties and maturation signaling to the cells [89–91]. However, to develop more appropriate universal bioinks, further studies are needed to improve the controllability over gelation and crosslinking kinetics as well as the mechanical properties of bioinks (e.g., stiffness and porosity) with a minimum need for customization by the end user [92]. Developing a universal bioink would significantly improve the reproducibility as well as decrease the time and costs of bioprinting.

5.1.1. Towards a universal bioink using decellularized-ECM

The majority of natural polymers like alginate, collagen, and fibrin lonely are not able to provide the complexity of the natural ECM

microenvironment for cell adherence, survival, and function. For example, alginate, a widely used hydrogel in bioprinting, lacks the complex cell-matrix interaction, and cell adherence or matrix degradation by the cells does not occur completely [93,94]. On the other hand, the mechanical properties of the lungs are affected by the ECM composition and abundance [95]. Therefore, dECM hydrogels offer considerable potentials to be used as a bioink to help recapitulate tissues and organs due to their cell and matrix level properties. At the cell level, dECM can modulate cell behavior such as cell attachment, migration, and differentiation and ensure the maintenance of selected cell functions and phenotypes [96,97]. At the matrix level, dECM ultrastructure and composition induce positive tissue organization [98] and promote constructive remodeling responses, as shown for a variety of tissues in both pre-clinical and clinical studies [99]. Also, dECM has suitable mechanical performance, similar to that of the native tissues. Human lung dECM hydrogels resembled the stiffness and viscoelasticity of the whole tissue when assessed with a low-load compression tester [100]. Furthermore, lung ECM hydrogels had protective effects on radiation-induced lung injury [101]. All of these findings show the advantages of the dECM and its potential to be used in lung and tracheal bioprinting.

dECM can be obtained by decellularizing tissues from humans or animals, e.g., cadaveric lungs from humans or pigs [102–106]. The obtained acellular lung scaffolds can be freeze-dried, powdered, and even combined with polymers like PCL and PEGDA to improve the physical integrity and promote the overall mechanical, structural, and geometrical properties of the printed construct at the macroscopic level [107]. The ECM components are detectable by proteomics [108–111]. To achieve repetitive results, automated decellularization devices with identical protocols can be applied. Automated decellularization devices have been developed and utilized for large lungs [112–114], removing the cells and DNA content while preserving the ECM components.

5.2. MSCs and iPSCs to functionalize 3D-printed lungs and trachea

Given the fact that over 40 different cell types need to be recapitulated to allow the engineered lungs to function properly [115], a reproducible source of stem cells is required to be differentiated and expanded to large cell numbers. Among various types of human pluripotent stem cells, MSCs and iPSCs have received considerable attention in tissue engineering and regenerative medicine [116]. Both MSCs and iPSCs have proved the ability to accelerate the neo-cartilage, neo-vasculature, and neo-epithelium formation in bioprinted tracheas or engineered lungs [21,63,64,117–119]. Also, autologous MSCs and iPSCs do not have the risk of immune rejection and bypass the ethical concerns that arise from the usage of embryonic stem cells [120,121]. Therefore, MSCs and iPSCs are an ideal cell source for bioprinting lungs and trachea.

Differentiation of stem cells in the bioprinted constructs can be controlled and directed during the construct culture and maturation [122]. One approach to direct stem cell differentiation to the desired cell phenotype would be utilizing soluble factors in the medium like the use of growth factors (e.g., transforming growth factor beta [TGF-β] and bone morphogenic proteins [BMPs]) and chemicals (e.g., dexamethasone and ascorbic acid) affecting MSC differentiation towards osteogenic or adipogenic lineage, for example [123]. When a bioprinted construct (a methacrylamide gelatin scaffold with bone mesenchymal stem cells [BMSCs]) was incubated in osteogenic medium for 14 days, a considerable increase in the expression of osteogenic reporter genes, such as osteocalcin, bone sialoprotein, and alkaline phosphatase was demonstrated, as compared to BMSCs kept in growth media [124]. Furthermore, to promote lineage commitment and maturation towards selected phenotypes, additives included into the bioink can be utilized. In a study, poly ethylene glycol (PEG), a bioinert polymer, was used to create osteogenic bioinks, and hyaluronic acid (HA) was added as a bone promoting additive. The MSCs printed within PEG-HA bioink showed greater osteogenic differentiation and increased collagen secretion for ECM remodeling [125]. Also, it has been shown that the surrounding ECM mechanical properties (e.g., substrate stiffness) and material composition affect stem cell fate and function [126]. When MSCs were seeded onto polyacrylamide gels coated with collagen I or fibronectin and of high, medium, and low elasticity, the MSCs were differentiated towards neurocytes, myocytes, and osteocytes, respectively [127,128].

Overall, MSCs and iPSCs have shown great potential for repopulating bioprinted constructs because of their expandability and multipotency. To control their differentiation, several approaches have been used such as the use of soluble factors in the medium, including additives into the bioink, and altering the surrounding ECM mechanical properties. More studies on the effect of growth factors and chemicals on the stem cell differentiation would better clarify the role of medium additives when maturing the 3DP constructs. Also, further studies are required on bioink properties as the right choice of bioink can promote the desired lineage commitment; dECM has been proved to include cues that facilitate the differentiation of the stem cells towards the resident cells of the tissue from which dECM was obtained [93,129,130]. All of these would help develop optimized and standardized bioprinting strategies to control the stem cells' differentiation towards the desired phenotypes in the engineered tissue constructs.

5.3. Bioprinters

Considering the complex architecture of the lungs, the research in pulmonary 3D bioprinting is currently limited to printing airways or large-scale models. For example, alveolar regions require creating a hollow structure with only a single cell size or a basement membrane layer of separation closely associated with convoluting microvessels, while maintaining a sealed air-fluid interface to avoid a gas embolism, and this requires bioprinting techniques with high resolution of printing.

Among available bioprinting techniques, extrusion and stereolithography are the most applicable methods for lung and tracheal bioprinting. The extrusion method has provided the resolution required for bioprinting tracheal grafts, but it is not high enough to print lung tissue parenchyma. At this time, the most promising method for lung parenchyma bioprinting is stereolithography. Stereolithography is a nozzle-free technique, providing high resolutions, and as the printing time is independent of the structure complexity, the print speed is high. On the other hand, while nozzle-based bioprinters retain their status in tracheal tissue engineering, stereolithography can also be applied for printing tracheas. This would facilitate producing an integrated lung and tracheal construct. Nonetheless, further efforts are needed to resolve current limitations of stereolithography regarding multicellular structure printing, limited applicability only for photo-crosslinking bioinks, and damage to the cells during photocuring or due to UV light toxicity.

5.4. Automated monitoring bioreactors: a system for 3D-printed construct maturation and a platform for pre-implant simulation

Engineered/bioprinted lungs and trachea will need a dynamic bioreactor capable of providing fluid and gas perfusion to mature the tissue or perform simulation before transplantation. Such bioreactors provide independent access lines through the vascular bed and airway compartments for oxygen and nutrition delivery and metabolic wastes removal. Bioreactors can provide maturation factors and physiological stimuli like perfusion and ventilation and then help mature the constructs. Providing such conditions in an automated manner increases the precision and repeatability of the results and decreases the time, costs, and risk of contamination [11,48,131]. On the other hand, monitoring bioreactors enable observation of biologically relevant parameters, such as O_2, pH, glucose, and lactate levels, in real-time and non-invasive manners, facilitating the way to control the culture conditions and obtain more mature lungs. For example, changes in oxygen uptake rates based on respiration activity [11] or dissolved oxygen measurements [132] during the whole lung culture helped estimate the metabolic states

and improve the proliferative phase of native or engineered lung tissues. Such monitoring bioreactors, therefore, can be applied to simulate the *in vivo* conditions and verify the bioprinted construct in terms of maturity and functionality before transplantation.

6. Conclusion

This paper reviews the achievements in lung and tracheal tissue engineering by 3D bioprinting. First, the criteria for lung and tracheal bioprinting are presented, including the scaffold design criteria, proper bioink properties, and applicable bioprinting techniques, showing the superiorities of stereolithography and extrusion bioprinting methods compared to other types of bioprinters for producing lungs and trachea. Then, the current progress in the application of 3D bioprinting in producing lung and tracheal tissues is discussed, exhibiting the accomplishments in alveoli-mimicking constructs (with the ability to oxygenate red blood cells) and tracheal grafts (implanted in small or large animal models) produced with or without polymers. However, despite all the progress, several limitations remain to achieve functional lung constructs by 3D bioprinting, including the use of soft bioinks, printing the hierarchical vascularization and architecture, and graded printing. Also, further investigations on producing a universal bioink with a focus on dECM, using MSCs and iPSCs, developing stereolithography bioprinting technique, and applying monitoring bioreactors would address these limitations and pave the way for reaching a nature-like printed construct. A combination of proper bioprinting techniques, bioinks with appropriate structural properties, and stem cells derived from patients would result in personalized 3DP whole lungs and trachea. Achieving such functional implantable constructs would change the paradigm of transplantation, reduce the cost burden of chronic pulmonary diseases, and significantly enhance public health in the future.

Declaration of competing interest

The authors declare that they have no known competing financial interests or personal relationships that could have appeared to influence the work reported in this paper.

Acknowledgments

The authors would like to appreciate the Research Center for New Technologies in Life Science Engineering of the University of Tehran for its scientific support. The corresponding author of this study would like to express his gratitude to Iran National Science Foundation (INSF) for supporting this research under grant number 78042095.

References

[1] WHO: Burden of COPD, World Heal, Organ, 2020, p. 1, accessed, https://www.who.int/respiratory/copd/burden/en/. (Accessed 25 May 2020).
[2] S.A. Quaderi, J.R. Hurst, The unmet global burden of COPD, Glob. Heal. Epidemiol. Genomics. 3 (2018) e4, https://doi.org/10.1017/gheg.2018.1.
[3] A.A. Pruitt, M.R. Rosenfeld, F. Graus, Neurological complications of solid organ transplantation, The Neurohospitalist 3 (2013) 152–166, https://doi.org/10.1177/1941874412466090.
[4] C.K. Black, K.M. Termanini, O. Aguirre, J.S. Hawksworth, M. Sosin, Solid organ transplantation in the 21st century, Ann. Transl. Med. 6 (2018), https://doi.org/10.21037/atm.2018.09.68, 409–409.
[5] T. Oto, L. Excell, A.P. Griffiths, B.J. Levvey, G.I. Snell, The implications of pulmonary embolism in a multiorgan donor for subsequent pulmonary, renal, and cardiac transplantation, J. Heart Lung Transplant. 27 (2008) 78–85, https://doi.org/10.1016/j.healun.2007.10.001.
[6] C.D. Spicer, Hydrogel scaffolds for tissue engineering: the importance of polymer choice, Polym. Chem. 11 (2020) 184–219, https://doi.org/10.1039/c9py01021a.
[7] I. Jun, H.S. Han, J.R. Edwards, H. Jeon, Electrospun fibrous scaffolds for tissue engineering: viewpoints on architecture and fabrication, Int. J. Mol. Sci. 19 (2018) 745, https://doi.org/10.3390/ijms19030745.
[8] M.P. Nikolova, M.S. Chavali, Recent advances in biomaterials for 3D scaffolds: a review, Bioact. Mater. 4 (2019) 271–292, https://doi.org/10.1016/j.bioactmat.2019.10.005.
[9] M. Li, M.J. Mondrinos, X. Chen, M.R. Gandhi, F.K. Ko, P.I. Lelkes, Co-electrospun poly(lactide-co-glycolide), gelatin, and elastin blends for tissue engineering scaffolds, J. Biomed. Mater. Res. 79 (2006) 963–973, https://doi.org/10.1002/jbm.a.30833.
[10] A. Doryab, M. Heydarian, G. Amoabediny, E. Sadroddiny, S. Mahfouzi, Recellularization on acellular lung tissue scaffold using perfusion-based bioreactor: an online monitoring strategy, J. Med. Biol. Eng. 37 (2017) 53–62, https://doi.org/10.1007/s40846-016-0205-1.
[11] S.H. Mahfouzi, G. Amoabediny, A. Doryab, S.H. Safiabadi-Tali, M. Ghanei, Noninvasive real-time assessment of cell viability in a three-dimensional tissue, Tissue Eng. C Methods 24 (2018) 197–204, https://doi.org/10.1089/ten.tec.2017.0371.
[12] J.J. Uriarte, F.E. Uhl, S.E. Rolandsson Enes, R.A. Pouliot, D.J. Weiss, Lung bioengineering: advances and challenges in lung decellularization and recellularization, Curr. Opin. Organ Transplant. 23 (2018) 673–678, https://doi.org/10.1097/MOT.0000000000000584.
[13] A. Jiao, N.E. Trosper, H.S. Yang, J. Kim, J.H. Tsui, S.D. Frankel, C.E. Murry, D.H. Kim, Thermoresponsive nanofabricated substratum for the engineering of three-dimensional tissues with layer-by-layer architectural control, ACS Nano 8 (2014) 4430–4439, https://doi.org/10.1021/nn4063962.
[14] P. Bajaj, R.M. Schweller, A. Khademhosseini, J.L. West, R. Bashir, 3D biofabrication strategies for tissue engineering and regenerative medicine, Annu. Rev. Biomed. Eng. 16 (2014) 247–276, https://doi.org/10.1146/annurev-bioeng-071813-105155.
[15] T. Lu, Y. Li, T. Chen, Techniques for fabrication and construction of three-dimensional scaffolds for tissue engineering, Int. J. Nanomed. 8 (2013) 337–350, https://doi.org/10.2147/IJN.S38635.
[16] E.S. Bishop, S. Mostafa, M. Pakvasa, H.H. Luu, M.J. Lee, J.M. Wolf, G.A. Ameer, T.C. He, R.R. Reid, 3-D bioprinting technologies in tissue engineering and regenerative medicine: current and future trends, Genes Dis 4 (2017) 185–195, https://doi.org/10.1016/j.gendis.2017.10.002.
[17] A.J. Broussard, S.M. Hall, M.G. Levitzky, Respiratory system. Essentials Pediatr. Anesthesiol., Elsevier, 2014, pp. 38–51, https://doi.org/10.1007/9781107375338.
[18] A. Hakim, O.S. Usmani, Structure of the lower respiratory tract. Ref. Modul. Biomed. Sci., Elsevier, 2014, https://doi.org/10.1016/b978-0-12-801238-3.00215-4.
[19] S.S. Rehmani, A.M. Al-Ayoubi, A. Ayub, M. Barsky, E. Lewis, R. Flores, R. Lebovics, F.Y. Bhora, Three-Dimensional-printed bioengineered tracheal grafts: preclinical results and potential for human use, Ann. Thorac. Surg. 104 (2017) 998–1004, https://doi.org/10.1016/j.athoracsur.2017.03.051.
[20] J.H. Park, J.K. Yoon, J.B. Lee, Y.M. Shin, K.W. Lee, S.W. Bae, J.H. Lee, J.J. Yu, C.R. Jung, Y.N. Youn, H.Y. Kim, D.H. Kim, Experimental tracheal replacement using 3-dimensional bioprinted artificial trachea with autologous epithelial cells and chondrocytes, Sci. Rep. 9 (2019) 2103, https://doi.org/10.1038/s41598-019-38565-z.
[21] S.W. Bae, K.W. Lee, J.H. Park, J.H. Lee, C.R. Jung, J.J. Yu, H.Y. Kim, D.H. Kim, 3D bioprinted artificial trachea with epithelial cells and chondrogenic-differentiated bone marrow-derived mesenchymal stem cells, Int. J. Mol. Sci. 19 (2018) 1624, https://doi.org/10.3390/ijms19061624.
[22] J.M. Townsend, L.M. Ott, J.R. Salash, K.M. Fung, J.T. Easley, H.B. Seim, J.K. Johnson, R.A. Weatherly, M.S. Detamore, Reinforced electrospun polycaprolactone nanofibers for tracheal repair in an in vivo ovine model, Tissue Eng. 24 (2018) 1301–1308, https://doi.org/10.1089/ten.tea.2017.0437.
[23] B. Grigoryan, S.J. Paulsen, D.C. Corbett, D.W. Sazer, C.L. Fortin, A.J. Zaita, P.T. Greenfield, N.J. Calafat, J.P. Gounley, A.H. Ta, F. Johansson, A. Randles, J.E. Rosenkrantz, J.D. Louis-Rosenberg, P.A. Galie, K.R. Stevens, J.S. Miller, Multivascular networks and functional intravascular topologies within biocompatible hydrogels, Science 364 (2019) 458–464, https://doi.org/10.1126/science.aav9750, 80-.
[24] J.A. Stramiello, R. Saddawi-Konefka, J. Ryan, M.T. Brigger, The role of 3D printing in pediatric airway obstruction: a systematic review, Int. J. Pediatr. Otorhinolaryngol. 132 (2020) 109923, https://doi.org/10.1016/j.ijporl.2020.109923.
[25] Z. Galliger, C.D. Vogt, A. Panoskaltsis-Mortari, 3D bioprinting for lungs and hollow organs, Transl. Res. 211 (2019) 19–34, https://doi.org/10.1016/j.trsl.2019.05.001.
[26] A. Makanya, A. Anagnostopoulou, V. Djonov, Development and remodeling of the vertebrate blood-gas barrier, BioMed Res. Int. 2013 (2013) 1–15, https://doi.org/10.1155/2013/101597.
[27] L. Knudsen, M. Ochs, The micromechanics of lung alveoli: structure and function of surfactant and tissue components, Histochem. Cell Biol. 150 (2018) 661–676, https://doi.org/10.1007/s00418-018-1747-9.
[28] A.A. Hislop, Airway and blood vessel interaction during lung development, J. Anat. 201 (2002) 325–334, https://doi.org/10.1046/j.1469-7580.2002.00097.x.
[29] R. Lanza, R. Langer, J.P. Vacanti, Principles of Tissue Engineering, fourth ed., Elsevier, 2013 https://doi.org/10.1016/C2011-0-07193-4.
[30] B. Suki, J.H.T. Bates, Extracellular matrix mechanics in lung parenchymal diseases, Respir. Physiol. Neurobiol. 163 (2008) 33–43, https://doi.org/10.1016/j.resp.2008.03.015.
[31] B. Suki, S. Ito, D. Stamenović, K.R. Lutchen, E.P. Ingenito, Invited review: biomechanics of the lung parenchyma: critical roles of collagen and mechanical forces, J. Appl. Physiol. 98 (2005) 1892–1899, https://doi.org/10.1152/japplphysiol.01087.2004.

[32] A. Shifren, R.P. Mecham, The stumbling block in lung repair of emphysema: elastic fiber assembly, Proc. Am. Thorac. Soc. 3 (2006) 428–433, https://doi.org/10.1513/pats.200601-009AW.

[33] B.E.M. Brand-Saberi, T. Schäfer, Trachea: anatomy and physiology, Thorac. Surg. Clin. 24 (2014) 1–5, https://doi.org/10.1016/j.thorsurg.2013.09.004.

[34] E.B. Hysinger, H.B. Panitch, Paediatric tracheomalacia, Paediatr. Respir. Rev. 17 (2016) 9–15, https://doi.org/10.1016/j.prrv.2015.03.002.

[35] L. Javia, M.A. Harris, S. Fuller, Rings, slings, and other tracheal disorders in the neonate, Semin. Fetal Neonatal Med. 21 (2016) 277–284, https://doi.org/10.1016/j.siny.2016.03.005.

[36] G. Amoabediny, N. Salehi-Nik, B. Heli, The role of biodegradable engineered scaffold in tissue engineering, Biomater. Sci. Eng. (2011) 153–172, https://doi.org/10.5772/24331.

[37] C.C.W. Hsia, D.M. Hyde, E.R. Weibel, Lung structure and the intrinsic challenges of gas exchange. Compr. Physiol., John Wiley & Sons, Inc., Hoboken, NJ, USA, 2016, pp. 827–895, https://doi.org/10.1002/cphy.c150028.

[38] L. Knudsen, M. Ochs, The micromechanics of lung alveoli: structure and function of surfactant and tissue components, Histochem. Cell Biol. 150 (2018) 661–676, https://doi.org/10.1007/s00418-018-1747-9.

[39] T. Chiang, V. Pepper, C. Best, E. Onwuka, C.K. Breuer, Clinical translation of tissue engineered trachea grafts, Ann. Otol. Rhinol. Laryngol. 125 (2016) 873–885, https://doi.org/10.1177/0003489416656646.

[40] D.J. Doyle, K.F. O'grady, Physics and modeling of the airway. Benumof Hagberg's Airw. Manag., Elsevier, 2013, pp. 92–117, https://doi.org/10.1016/b978-1-4377-2764-7.00004-x, e2.

[41] D. Sicard, A.J. Haak, K.M. Choi, A.R. Craig, L.E. Fredenburgh, D.J. Tschumperlin, Aging and anatomical variations in lung tissue stiffness, Am. J. Physiol. Lung Cell Mol. Physiol. 314 (2018) L946–L955, https://doi.org/10.1152/ajplung.00415.2017.

[42] C.B. Raub, A.J. Putnam, B.J. Tromberg, S.C. George, Predicting bulk mechanical properties of cellularized collagen gels using multiphoton microscopy, Acta Biomater. 6 (2010) 4657–4665, https://doi.org/10.1016/j.actbio.2010.07.004.

[43] S.S. Soofi, J.A. Last, S.J. Liliensiek, P.F. Nealey, C.J. Murphy, The elastic modulus of Matrigel™ as determined by atomic force microscopy, J. Struct. Biol. 167 (2009) 216–219, https://doi.org/10.1016/j.jsb.2009.05.005.

[44] M. Ahearne, Y. Yang, A.J. El Haj, K.Y. Then, K.K. Liu, Characterizing the viscoelastic properties of thin hydrogel-based constructs for tissue engineering applications, J. R. Soc. Interface 2 (2005) 455–463, https://doi.org/10.1098/rsif.2005.0065.

[45] M.M. De Santis, D.A. Bölükbas, S. Lindstedt, D.E. Wagner, How to build a lung: latest advances and emerging themes in lung bioengineering, Eur. Respir. J. 52 (2018), https://doi.org/10.1183/13993003.01355-2016.

[46] M. Zhu, Y. Wang, G. Ferracci, J. Zheng, N.J. Cho, B.H. Lee, Gelatin methacryloyl and its hydrogels with an exceptional degree of controllability and batch-to-batch consistency, Sci. Rep. 9 (2019) 6863, https://doi.org/10.1038/s41598-019-42186-x.

[47] C. Mandrycky, Z. Wang, K. Kim, D.H. Kim, 3D bioprinting for engineering complex tissues, Biotechnol. Adv. 34 (2016) 422–434, https://doi.org/10.1016/j.biotechadv.2015.12.011.

[48] S.V. Murphy, A. Atala, 3D bioprinting of tissues and organs, Nat. Biotechnol. 32 (2014) 773–785, https://doi.org/10.1038/nbt.2958.

[49] K.C. Hribar, P. Soman, J. Warner, P. Chung, S. Chen, Light-assisted direct-write of 3D functional biomaterials, Lab Chip 14 (2014) 268–275, https://doi.org/10.1039/c3lc50634g.

[50] S. Derakhshanfar, R. Mbeleck, K. Xu, X. Zhang, W. Zhong, M. Xing, 3D bioprinting for biomedical devices and tissue engineering: a review of recent trends and advances, Bioact. Mater. 3 (2018) 144–156, https://doi.org/10.1016/j.bioactmat.2017.11.008.

[51] I.T. Ozbolat, Y. Yu, Bioprinting toward organ fabrication: challenges and future trends, IEEE Trans. Biomed. Eng. 60 (2013) 691–699, https://doi.org/10.1109/TBME.2013.2243912.

[52] N. Merna, K.M. Fung, J.J. Wang, C.R. King, K.C. Hansen, K.L. Christman, S.C. George, Differential β3 integrin expression regulates the response of human lung and cardiac fibroblasts to extracellular matrix and its components, Tissue Eng. 21 (2015) 2195–2205, https://doi.org/10.1089/ten.tea.2014.0337.

[53] K. Nair, M. Gandhi, S. Khalil, K.C. Yan, M. Marcolongo, K. Barbee, W. Sun, Characterization of cell viability during bioprinting processes, Biotechnol. J. 4 (2009) 1168–1177, https://doi.org/10.1002/biot.200900004.

[54] A. Munaz, R.K. Vadivelu, J. St John, M. Barton, H. Kamble, N.T. Nguyen, Three-dimensional printing of biological matters, J. Sci. Adv. Mater. Devices. 1 (2016) 1–17, https://doi.org/10.1016/j.jsamd.2016.04.001.

[55] E.R. Weibel, Morphological basis of alveolar-capillary gas exchange, Physiol. Rev. 53 (1973) 419–495, https://doi.org/10.1152/physrev.1973.53.2.419.

[56] M. Ochs, J.R. Nyengaard, A. Jung, L. Knudsen, M. Voigt, T. Wahlers, J. Richter, H.J.G. Gundersen, The number of alveoli in the human lung, Am. J. Respir. Crit. Care Med. 169 (2004) 120–124, https://doi.org/10.1164/rccm.200308-1107oc.

[57] C.G. Plopper, J.R. Harkema, The respiratory system and its use in research. Lab. Primate, Elsevier, 2005, pp. 503–526, https://doi.org/10.1016/B978-012080261-6/50030-1.

[58] L. Horvath, Y. Umehara, C. Jud, F. Blank, A. Petri-Fink, B. Rothen-Rutishauser, Engineering an in vitro air-blood barrier by 3D bioprinting, Sci. Rep. 5 (2015), https://doi.org/10.1038/srep07974.

[59] G. Krasteva, B.J. Canning, P. Hartmann, T.Z. Veres, T. Papadakis, C. Mühlfeld, K. Schliecker, Y.N. Tallini, A. Braun, H. Hackstein, N. Baal, E. Weihe, B. Schütz, M. Kotlikoff, I. Ibanez-Tallon, W. Kummer, Cholinergic chemosensory cells in the trachea regulate breathing, Proc. Natl. Acad. Sci. U.S.A. 108 (2011) 9478–9483, https://doi.org/10.1073/pnas.1019418108.

[60] D. Xia, D. Jin, Q. Wang, M. Gao, J. Zhang, H. Zhang, J. Bai, B. Feng, M. Chen, Y. Huang, Y. Zhong, N. Witman, W. Wang, Z. Xu, H. Zhang, M. Yin, W. Fu, Tissue-engineered trachea from a 3D-printed scaffold enhances whole-segment tracheal repair in a goat model, J. Tissue Eng. Regen. Med. 13 (2019) 694–703, https://doi.org/10.1002/term.2828.

[61] R. Song, M. Murphy, C. Li, K. Ting, C. Soo, Z. Zheng, Current development of biodegradable polymeric materials for biomedical applications, Drug Des. Dev. Ther. 12 (2018) 3117–3145, https://doi.org/10.2147/DDDT.S165440.

[62] K. Rezwan, Q.Z. Chen, J.J. Blaker, A.R. Boccaccini, Biodegradable and bioactive porous polymer/inorganic composite scaffolds for bone tissue engineering, Biomaterials 27 (2006) 3413–3431, https://doi.org/10.1016/j.biomaterials.2006.01.039.

[63] J.W. Chang, S.A. Park, J.K. Park, J.W. Choi, Y.S. Kim, Y.S. Shin, C.H. Kim, Tissue-engineered tracheal reconstruction using three-dimensionally printed artificial tracheal graft: preliminary report, Artif. Organs 38 (2014), https://doi.org/10.1111/aor.12310.

[64] J.H. Park, J.Y. Park, I.C. Nam, S.H. Hwang, C.S. Kim, J.W. Jung, J. Jang, H. Lee, Y. Choi, S.H. Park, S.W. Kim, D.W. Cho, Human turbinate mesenchymal stromal cell sheets with bellows graft for rapid tracheal epithelial regeneration, Acta Biomater. 25 (2015) 56–64, https://doi.org/10.1016/j.actbio.2015.07.014.

[65] R. Kaye, T. Goldstein, D.A. Grande, D. Zeltsman, L.P. Smith, A 3-dimensional bioprinted tracheal segment implant pilot study: rabbit tracheal resection with graft implantation, Int. J. Pediatr. Otorhinolaryngol. 117 (2019) 175–178, https://doi.org/10.1016/j.ijporl.2018.11.010.

[66] J.Y. Lee, J.H. Park, M.J. Ahn, S.W. Kim, D.W. Cho, Long-term study on off-the-shelf tracheal graft: a conceptual approach for urgent implantation, Mater. Des. 185 (2020) 108218, https://doi.org/10.1016/j.matdes.2019.108218.

[67] Y. Shan, Y. Wang, J. Li, H. Shi, Y. Fan, J. Yang, W. Ren, X. Yu, Biomechanical properties and cellular biocompatibility of 3D printed tracheal graft, Bioproc. Biosyst. Eng. 40 (2017) 1813–1823, https://doi.org/10.1007/s00449-017-1835-6.

[68] D. Ke, H. Yi, S. Est-Witte, S. George, C. Kengla, S.J. Lee, A. Atala, S.V. Murphy, Bioprinted trachea constructs with patient-matched design, mechanical and biological properties, Biofabrication 12 (2020), 015022, https://doi.org/10.1088/1758-5090/ab5354.

[69] T.A. Goldstein, B.D. Smith, D. Zeltsman, D. Grande, L.P. Smith, Introducing a 3-dimensionally printed, tissue-engineered graft for airway reconstruction: a pilot study, Otolaryngol. Head Neck Surg. 153 (2015) 1001–1006, https://doi.org/10.1177/0194599815605492.

[70] J.H. Park, J.M. Hong, Y.M. Ju, J.W. Jung, H.W. Kang, S.J. Lee, J.J. Yoo, S.W. Kim, S.H. Kim, D.W. Cho, A novel tissue-engineered trachea with a mechanical behavior similar to native trachea, Biomaterials 62 (2015) 106–115, https://doi.org/10.1016/j.biomaterials.2015.05.008.

[71] C.A. Best, V.K. Pepper, D. Ohst, K. Bodnyk, E. Heuer, E.A. Onwuka, N. King, R. Strouse, J. Grischkan, C.K. Breuer, J. Johnson, T. Chiang, Designing a tissue-engineered tracheal scaffold for preclinical evaluation, Int. J. Pediatr. Otorhinolaryngol. 104 (2018) 155–160, https://doi.org/10.1016/j.ijporl.2017.10.036.

[72] S.Y. Jung, S.J. Lee, H.Y. Kim, H.S. Park, Z. Wang, H.J. Kim, J.J. Yoo, S.M. Chung, H.S. Kim, 3D printed polyurethane prosthesis for partial tracheal reconstruction: a pilot animal study, Biofabrication 8 (2016) 1–10, https://doi.org/10.1088/1758-5090/8/4/045015.

[73] A. Dehghanifard, M. Shahjahani, M. Soleimani, N. Saki, The emerging role of mesenchymal stem cells in tissue engineering, Int. J. Hematol. Stem Cell Res. 7 (2013) 43–44.

[74] D. Taniguchi, K. Matsumoto, T. Tsuchiya, R. MacHino, Y. Takeoka, A. Elgalad, K. Gunge, K. Takagi, Y. Taura, G. Hatachi, N. Matsuo, N. Yamasaki, K. Nakayama, T. Nagayasu, Scaffold-free trachea regeneration by tissue engineering with bio-3D printing, Interact. Cardiovasc. Thorac. Surg. 26 (2018) 745–752, https://doi.org/10.1093/icvts/ivx444.

[75] R. Machino, K. Matsumoto, D. Taniguchi, T. Tsuchiya, Y. Takeoka, Y. Taura, M. Moriyama, T. Tetsuo, S. Oyama, K. Takagi, T. Miyazaki, G. Hatachi, R. Doi, K. Shimoyama, N. Matsuo, N. Yamasaki, K. Nakayama, T. Nagayasu, Replacement of rat tracheas by layered, trachea-like, scaffold-free structures of human cells using a bio-3D printing system, Adv. Healthc. Mater. 8 (2019) 1800983, https://doi.org/10.1002/adhm.201800983.

[76] G. Cidonio, M. Glinka, J.I. Dawson, R.O.C. Oreffo, The cell in the ink: improving biofabrication by printing stem cells for skeletal regenerative medicine, Biomaterials 209 (2019) 10–24, https://doi.org/10.1016/j.biomaterials.2019.04.009.

[77] E.R. Weibel, Lung morphometry: the link between structure and function, Cell Tissue Res. 367 (2017) 413–426, https://doi.org/10.1007/s00441-016-2541-4.

[78] T.J. Hinton, Q. Jallerat, R.N. Palchesko, J.H. Park, M.S. Grodzicki, H.J. Shue, M.H. Ramadan, A.R. Hudson, A.W. Feinberg, Three-dimensional printing of complex biological structures by freeform reversible embedding of suspended hydrogels, Sci. Adv. 1 (2015), e1500758, https://doi.org/10.1126/sciadv.1500758.

[79] T.J. Hinton, A. Lee, A.W. Feinberg, 3D bioprinting from the micrometer to millimeter length scales: size does matter, Curr. Opin. Biomed. Eng. 1 (2017) 31–37, https://doi.org/10.1016/j.cobme.2017.02.004.

[80] W. Wu, A. Deconinck, J.A. Lewis, Omnidirectional printing of 3D microvascular networks, Adv. Mater. 23 (2011) 178–183, https://doi.org/10.1002/adma.201004625.

[81] D.B. Kolesky, K.A. Homan, M.A. Skylar-Scott, J.A. Lewis, Three-dimensional bioprinting of thick vascularized tissues, Proc. Natl. Acad. Sci. U.S.A. 113 (2016) 3179–3184, https://doi.org/10.1073/pnas.1521342113.

[82] D.B. Kolesky, R.L. Truby, A.S. Gladman, T.A. Busbee, K.A. Homan, J.A. Lewis, 3D bioprinting of vascularized, heterogeneous cell-laden tissue constructs, Adv. Mater. 26 (2014) 3124–3130, https://doi.org/10.1002/adma.201305506.

[83] T.J. Ober, D. Foresti, J.A. Lewis, Active mixing of complex fluids at the microscale, Proc. Natl. Acad. Sci. U.S.A. 112 (2015) 12293–12298, https://doi.org/10.1073/pnas.1509224112.

[84] K.E. Drzewiecki, J.N. Malavade, I. Ahmed, C.J. Lowe, D.I. Shreiber, A thermoreversible, photocrosslinkable collagen bio-ink for free-form fabrication of scaffolds for regenerative medicine, Technology (2017) 185–195, https://doi.org/10.1142/s2339547817500091, 05.

[85] J.W. Nichol, S.T. Koshy, H. Bae, C.M. Hwang, S. Yamanlar, A. Khademhosseini, Cell-laden microengineered gelatin methacrylate hydrogels, Biomaterials 31 (2010) 5536–5544, https://doi.org/10.1016/j.biomaterials.2010.03.064.

[86] L. Elomaa, E. Keshi, I.M. Sauer, M. Weinhart, Development of GelMA/PCL and dECM/PCL resins for 3D printing of acellular in vitro tissue scaffolds by stereolithography, Mater. Sci. Eng. C 112 (2020) 110958, https://doi.org/10.1016/j.msec.2020.110958.

[87] W. Zhu, H. Cui, B. Boualam, F. Masood, E. Flynn, R.D. Rao, Z.Y. Zhang, L.G. Zhang, 3D bioprinting mesenchymal stem cell-laden construct with core-shell nanospheres for cartilage tissue engineering, Nanotechnology 29 (2018) 185101, https://doi.org/10.1088/1361-6528/aaafa1.

[88] S.S. Mahdavi, M.J. Abdekhodaie, H. Kumar, S. Mashayekhan, A. Baradaran-Rafii, K. Kim, Stereolithography 3D bioprinting method for fabrication of human corneal stroma equivalent, Ann. Biomed. Eng. 48 (2020), https://doi.org/10.1007/s10439-020-02537-6, 1955–1970.

[89] S.V. Murphy, A. Skardal, L. Song, K. Sutton, R. Haug, D.L. Mack, J. Jackson, S. Soker, A. Atala, Solubilized amnion membrane hyaluronic acid hydrogel accelerates full-thickness wound healing, Stem Cells Transl. Med. 6 (2017) 2020–2032, https://doi.org/10.1002/sctm.17-0053.

[90] M. Devarasetty, E. Wang, S. Soker, A. Skardal, Mesenchymal stem cells support growth and organization of host-liver colorectal-tumor organoids and possibly resistance to chemotherapy, Biofabrication 9 (2017), 021002, https://doi.org/10.1088/1758-5090/aa7484.

[91] A. Skardal, M. Devarasetty, H.W. Kang, I. Mead, C. Bishop, T. Shupe, S.J. Lee, J. Jackson, J. Yoo, S. Soker, A. Atala, A hydrogel bioink toolkit for mimicking native tissue biochemical and mechanical properties in bioprinted tissue constructs, Acta Biomater. 25 (2015) 24–34, https://doi.org/10.1016/j.actbio.2015.07.030.

[92] A. Skardal, Perspective: "Universal" bioink technology for advancing extrusion bioprinting-based biomanufacturing, Bioprinting 10 (2018), e00026, https://doi.org/10.1016/j.bprint.2018.e00026.

[93] F. Pati, J. Jang, D.H. Ha, S. Won Kim, J.W. Rhie, J.H. Shim, D.H. Kim, D.W. Cho, Printing three-dimensional tissue analogues with decellularized extracellular matrix bioink, Nat. Commun. 5 (2014) 3935, https://doi.org/10.1038/ncomms4935.

[94] N.E. Fedorovich, J. Alblas, J.R. De Wijn, W.E. Hennink, A.B.J. Verbout, W.J.A. Dhert, Hydrogels as extracellular matrices for skeletal tissue engineering: state-of-the-art and novel application in organ printing, Tissue Eng. 13 (2007) 1905–1925, https://doi.org/10.1089/ten.2006.0175.

[95] A.J. Haak, Q. Tan, D.J. Tschumperlin, Matrix biomechanics and dynamics in pulmonary fibrosis, Matrix Biol. 73 (2018) 64–76, https://doi.org/10.1016/j.matbio.2017.12.004.

[96] K.H. Nakayama, C.C.I. Lee, C.A. Batchelder, A.F. Tarantal, Tissue specificity of decellularized rhesus monkey kidney and lung scaffolds, PloS One 8 (2013), https://doi.org/10.1371/journal.pone.0064134.

[97] E. Garreta, L. de Oñate, M.E. Fernández-Santos, R. Oria, C. Tarantino, A.M. Climent, A. Marco, M. Samitier, E. Martínez, M. Valls-Margarit, R. Matesanz, D.A. Taylor, F. Fernández-Avilés, J.C. Izpisua Belmonte, N. Montserrat, Myocardial commitment from human pluripotent stem cells: rapid production of human heart grafts, Biomaterials 98 (2016) 64–78, https://doi.org/10.1016/j.biomaterials.2016.04.003.

[98] S.F. Badylak, D. Taylor, K. Uygun, Whole-organ tissue engineering: decellularization and recellularization of three-dimensional matrix scaffolds, Annu. Rev. Biomed. Eng. 13 (2011) 27–53, https://doi.org/10.1146/annurev-bioeng-071910-124743.

[99] S.F. Badylak, J.L. Dziki, B.M. Sicari, F. Ambrosio, M.L. Boninger, Mechanisms by which acellular biologic scaffolds promote functional skeletal muscle restoration, Biomaterials 103 (2016) 128–136, https://doi.org/10.1016/j.biomaterials.2016.06.047.

[100] R.H.J. de Hilster, P.K. Sharma, M.R. Jonker, E.S. White, E.A. Gercama, M. Roobeek, W. Timens, M.C. Harmsen, M.N. Hylkema, J.K. Burgess, Human lung extracellular matrix hydrogels resemble the stiffness and viscoelasticity of native lung tissue, Am. J. Physiol. Lung Cell Mol. Physiol. 318 (2020) L698–L704, https://doi.org/10.1152/ajplung.00451.2019.

[101] J. Zhou, P. Wu, H. Sun, H. Zhou, Y. Zhang, Z. Xiao, Lung tissue extracellular matrix-derived hydrogels protect against radiation-induced lung injury by suppressing epithelial–mesenchymal transition, J. Cell. Physiol. 235 (2020) 2377–2388, https://doi.org/10.1002/jcp.29143.

[102] X. Ren, P.T. Moser, S.E. Gilpin, T. Okamoto, T. Wu, L.F. Tapias, F.E. Mercier, L. Xiong, R. Ghawi, D.T. Scadden, D.J. Mathisen, H.C. Ott, Engineering pulmonary vasculature in decellularized rat and human lungs, Nat. Biotechnol. 33 (2015) 1097–1102, https://doi.org/10.1038/nbt.3354.

[103] S. Geerts, S. Ozer, M. Jaramillo, M.L. Yarmush, B.E. Uygun, Nondestructive methods for monitoring cell removal during rat liver decellularization, Tissue Eng. C Methods 22 (2016) 671–678, https://doi.org/10.1089/ten.tec.2015.0571.

[104] J.D. O'Neill, R. Anfang, A. Anandappa, J. Costa, J. Javidfar, H.M. Wobma, G. Singh, D.O. Freytes, M.D. Bacchetta, J.R. Sonett, G. Vunjak-Novakovic, Decellularization of human and porcine lung tissues for pulmonary tissue engineering, Ann. Thorac. Surg. 96 (2013) 1046–1056, https://doi.org/10.1016/j.athoracsur.2013.04.022.

[105] S. Zia, M. Mozafari, G. Natasha, A. Tan, Z. Cui, A.M. Seifalian, Hearts beating through decellularized scaffolds: whole-organ engineering for cardiac regeneration and transplantation, Crit. Rev. Biotechnol. 36 (2016) 705–715, https://doi.org/10.3109/07388551.2015.1007495.

[106] M.F.M. Gerli, J.P. Guyette, D. Evangelista-Leite, B.B. Ghoshhajra, H.C. Ott, Perfusion decellularization of a human limb: a novel platform for composite tissue engineering and reconstructive surgery, PloS One 13 (2018), e0191497, https://doi.org/10.1371/journal.pone.0191497.

[107] S.V. Murphy, P. De Coppi, A. Atala, Opportunities and challenges of translational 3D bioprinting, Nat. Biomed. Eng. 4 (2020) 370–380, https://doi.org/10.1038/s41551-019-0471-7.

[108] A. Byron, J.D. Humphries, M.J. Humphries, Defining the extracellular matrix using proteomics, Int. J. Exp. Pathol. 94 (2013) 75–92, https://doi.org/10.1111/iep.12011.

[109] A. Naba, K.R. Clauser, D.R. Mani, S.A. Carr, R.O. Hynes, Quantitative proteomic profiling of the extracellular matrix of pancreatic islets during the angiogenic switch and insulinoma progression, Sci. Rep. 7 (2017) 40495, https://doi.org/10.1038/srep40495.

[110] A. Naba, K.R. Clauser, H. Ding, C.A. Whittaker, S.A. Carr, R.O. Hynes, The extracellular matrix: tools and insights for the "omics" era, Matrix Biol. 49 (2016) 10–24, https://doi.org/10.1016/j.matbio.2015.06.003.

[111] E.T. Goddard, R.C. Hill, A. Barrett, C. Betts, Q. Guo, O. Maller, V.F. Borges, K.C. Hansen, P. Schedin, Quantitative extracellular matrix proteomics to study mammary and liver tissue microenvironments, Int. J. Biochem. Cell Biol. 81 (2016) 223–232, https://doi.org/10.1016/j.biocel.2016.10.014.

[112] Z. Khalpey, N. Qu, C. Hemphill, A.V. Louis, A.S. Ferng, T.G. Son, K. Stavoe, K. Penick, P.L. Tran, J. Konhilas, D.S. Lagrand, J.G.N. Garcia, Rapid porcine lung decellularization using a novel organ regenerative control acquisition bioreactor, Am. Soc. Artif. Intern. Organs J. 61 (2015) 71–77, https://doi.org/10.1097/MAT.0000000000000159.

[113] A.P. Price, L.M. Godin, A. Domek, T. Cotter, J. D'Cunha, D.A. Taylor, A. Panoskaltsis-Mortari, Automated Decellularization of Intact, Human-Sized Lungs for Tissue Engineering, 2015, https://doi.org/10.1089/ten.tec.2013.0756.

[114] J.E. Nichols, J. Niles, M. Riddle, G. Vargas, T. Schilagard, L. Ma, K. Edward, S. La Francesca, J. Sakamoto, S. Vega, M. Ogadegbe, R. Mlcak, D. Deyo, L. Woodson, C. Mcquitty, S. Lick, D. Beckles, E. Melo, J. Cortiella, Production and assessment of decellularized pig and human lung scaffolds, Tissue Eng. 19 (2013) 2045–2062, https://doi.org/10.1089/ten.tea.2012.0250.

[115] T.J. Franks, T.V. Colby, W.D. Travis, R.M. Tuder, H.Y. Reynolds, A.R. Brody, W.V. Cardoso, R.G. Crystal, C.J. Drake, J. Engelhardt, M. Frid, E. Herzog, R. Mason, S.H. Phan, S.H. Randell, M.C. Rose, T. Stevens, J. Serge, M.E. Sunday, J.A. Voynow, B.M. Weinstein, J. Whitsett, M.C. Williams, Resident cellular components of the human lung current knowledge and goals for research on cell phenotyping and function, Proc. Am. Thorac. Soc. 5 (2008) 763–766, https://doi.org/10.1513/pats.200803-025HR.

[116] S. Derakhti, S.H. Safiabadi-Tali, G. Amoabediny, M. Sheikhpour, Attachment and detachment strategies in microcarrier-based cell culture technology: a comprehensive review, Mater. Sci. Eng. C 103 (2019) 109782, https://doi.org/10.1016/j.msec.2019.109782.

[117] M. Ghaedi, E.A. Calle, J.J. Mendez, A.L. Gard, J. Balestrini, A. Booth, P.F. Bove, L. Gui, E.S. White, L.E. Niklason, Human iPS cell-derived alveolar epithelium repopulates lung extracellular matrix, J. Clin. Invest. 123 (2013) 4950–4962, https://doi.org/10.1172/JCI68793.

[118] S.E. Gilpin, X. Ren, T. Okamoto, J.P. Guyette, H. Mou, J. Rajagopal, D.J. Mathisen, J.P. Vacanti, H.C. Ott, Enhanced lung epithelial specification of human induced pluripotent stem cells on decellularized lung matrix, Ann. Thorac. Surg. 98 (2014) 1721–1729, https://doi.org/10.1016/j.athoracsur.2014.05.080.

[119] M. Ghaedi, A.V. Le, G. Hatachi, A. Beloiartsev, K. Rocco, A. Sivarapatna, J.J. Mendez, P. Baevova, R.N. Dyal, K.L. Leiby, E.S. White, L.E. Niklason, Bioengineered lungs generated from human iPSCs-derived epithelial cells on native extracellular matrix, J. Tissue Eng. Regen. Med. 12 (2018) e1623–e1635, https://doi.org/10.1002/term.2589.

[120] H.D. Zomer, A.S. Vidane, N.N. Gonçalves, C.E. Ambrósio, Mesenchymal and induced pluripotent stem cells: general insights and clinical perspectives, Stem Cells Cloning, Adv. Appl. 8 (2015) 125–134, https://doi.org/10.2147/SCCAA.S88036.

[121] A.A. Dayem, S. Bin Lee, K. Kim, K.M. Lim, T. Il Jeon, J. Seok, S.G. Cho, Production of mesenchymal stem cells through stem cell reprogramming, Int. J. Mol. Sci. 20 (2019) 1922, https://doi.org/10.3390/ijms20081922.

[122] K. Kolind, K.W. Leong, F. Besenbacher, M. Foss, Guidance of stem cell fate on 2D patterned surfaces, Biomaterials 33 (2012) 6626–6633, https://doi.org/10.1016/j.biomaterials.2012.05.070.

[123] S. Ding, P.G. Schultz, A role for chemistry in stem cell biology, Nat. Biotechnol. 22 (2004) 833–840, https://doi.org/10.1038/nbt987.

[124] M. Du, B. Chen, Q. Meng, S. Liu, X. Zheng, C. Zhang, H. Wang, H. Li, N. Wang, J. Dai, 3D bioprinting of BMSC-laden methacrylamide gelatin scaffolds with CBD-BMP2-collagen microfibers, Biofabrication 7 (2015), 044104, https://doi.org/10.1088/1758-5090/7/4/044104.

[125] G. Gao, X. Cui, Three-dimensional bioprinting in tissue engineering and regenerative medicine, Biotechnol. Lett. 38 (2016) 203–211, https://doi.org/10.1007/s10529-015-1975-1.
[126] S.W. Lane, D.A. Williams, F.M. Watt, Modulating the stem cell niche for tissue regeneration, Nat. Biotechnol. 32 (2014) 795–803, https://doi.org/10.1038/nbt.2978.
[127] A.S. Rowlands, P.A. George, J.J. Cooper-White, Directing osteogenic and myogenic differentiation of MSCs: interplay of stiffness and adhesive ligand presentation, Am. J. Physiol. Cell Physiol. 295 (2008) C1037–C1044, https://doi.org/10.1152/ajpcell.67.2008.
[128] A.J. Engler, S. Sen, H.L. Sweeney, D.E. Discher, Matrix elasticity directs stem cell lineage specification, Cell 126 (2006) 677–689, https://doi.org/10.1016/j.cell.2006.06.044.
[129] S.L.J. Ng, K. Narayanan, S. Gao, A.C.A. Wan, Lineage restricted progenitors for the repopulation of decellularized heart, Biomaterials 32 (2011) 7571–7580, https://doi.org/10.1016/j.biomaterials.2011.06.065.
[130] F. Gattazzo, A. Urciuolo, P. Bonaldo, Extracellular matrix: a dynamic microenvironment for stem cell niche, Biochim. Biophys. Acta Gen. Subj. 1840 (2014) 2506–2519, https://doi.org/10.1016/j.bbagen.2014.01.010.
[131] A. Panoskaltsis-Mortari, Bioreactor development for lung tissue engineering, Curr. Transplant. Reports 2 (2015) 90–97, https://doi.org/10.1007/s40472-014-0048-z.
[132] A.J. Engler, A.V. Le, P. Baevova, L.E. Niklason, Controlled gas exchange in whole lung bioreactors, J. Tissue Eng. Regen. Med. 12 (2018), https://doi.org/10.1002/term.2408 e119–e129.
[133] S. Michael, H. Sorg, C.T. Peck, L. Koch, A. Deiwick, B. Chichkov, P.M. Vogt, K. Reimers, Tissue engineered skin substitutes created by laser-assisted bioprinting form skin-like structures in the dorsal skin fold chamber in mice, PloS One 8 (2013), e57741, https://doi.org/10.1371/journal.pone.0057741.
[134] L. Koch, S. Kuhn, H. Sorg, M. Gruene, S. Schlie, R. Gaebel, B. Polchow, K. Reimers, S. Stoelting, N. Ma, P.M. Vogt, G. Steinhoff, B. Chichkov, Laser printing of skin cells and human stem cells, Tissue Eng. C Methods 16 (2010) 847–854, https://doi.org/10.1089/ten.tec.2009.0397.
[135] S.V. Murphy, A. Skardal, A. Atala, Evaluation of hydrogels for bio-printing applications, J. Biomed. Mater. Res. 101 A (2013) 272–284, https://doi.org/10.1002/jbm.a.34326.
[136] H. Cui, M. Nowicki, J.P. Fisher, L.G. Zhang, 3D bioprinting for organ regeneration, Adv. Healthc. Mater. 6 (2017) 1601118, https://doi.org/10.1002/adhm.201601118.
[137] E. Garreta, R. Oria, C. Tarantino, M. Pla-Roca, P. Prado, F. Fernández-Avilés, J.M. Campistol, J. Samitier, N. Montserrat, Tissue engineering by decellularization and 3D bioprinting, Mater. Today 20 (2017) 166–178, https://doi.org/10.1016/j.mattod.2016.12.005.
[138] T. Xu, J. Jin, C. Gregory, J.J. Hickman, T. Boland, Inkjet printing of viable mammalian cells, Biomaterials 26 (2005) 93–99, https://doi.org/10.1016/j.biomaterials.2004.04.011.
[139] S. Catros, B. Guillotin, M. Bačáková, J.C. Fricain, F. Guillemot, Effect of laser energy, substrate film thickness and bioink viscosity on viability of endothelial cells printed by laser-assisted bioprinting, Appl. Surf. Sci. 257 (2011) 5142–5147, https://doi.org/10.1016/j.apsusc.2010.11.049.
[140] R. Chang, J. Nam, W. Sun, Effects of dispensing pressure and nozzle diameter on cell survival from solid freeform fabrication-based direct cell writing, Tissue Eng. 14 (2008) 41–48, https://doi.org/10.1089/ten.a.2007.0004.
[141] C. Shuai, S. Duan, P. Wu, D. Gao, P. Feng, C. Gao, S. Peng, Development of bioceramic bone scaffolds by introducing triple liquid phases, J. Mater. Res. 31 (2016) 3498–3505, https://doi.org/10.1557/jmr.2016.356.
[142] K. Liu, H. Sun, Y. Shi, J. Liu, S. Zhang, S. Huang, M. Wang, Research on selective laser sintering of Kaolin-epoxy resin ceramic powders combined with cold isostatic pressing and sintering, Ceram. Int. 42 (2016) 10711–10718, https://doi.org/10.1016/j.ceramint.2016.03.190.
[143] C.C. Chang, E.D. Boland, S.K. Williams, J.B. Hoying, Direct-write bioprinting three-dimensional biohybrid systems for future regenerative therapies, J. Biomed. Mater. Res. B Appl. Biomater. 98 B (2011) 160–170, https://doi.org/10.1002/jbm.b.31831.
[144] F. Guillemot, A. Souquet, S. Catros, B. Guillotin, J. Lopez, M. Faucon, B. Pippenger, R. Bareille, M. Rémy, S. Bellance, P. Chabassier, J.C. Fricain, J. Amédée, High-throughput laser printing of cells and biomaterials for tissue engineering, Acta Biomater. 6 (2010) 2494–2500, https://doi.org/10.1016/j.actbio.2009.09.029.
[145] P.G. Campbell, E.D. Miller, G.W. Fisher, L.M. Walker, L.E. Weiss, Engineered spatial patterns of FGF-2 immobilized on fibrin direct cell organization, Biomaterials 26 (2005) 6762–6770, https://doi.org/10.1016/j.biomaterials.2005.04.032.
[146] J.A. Phillippi, E. Miller, L. Weiss, J. Huard, A. Waggoner, P. Campbell, Microenvironments engineered by inkjet bioprinting spatially direct adult stem cells toward muscle- and bone-like subpopulations, Stem Cell. 26 (2008) 127–134, https://doi.org/10.1634/stemcells.2007-0520.
[147] Z. Wang, R. Abdulla, B. Parker, R. Samanipour, S. Ghosh, K. Kim, A simple and high-resolution stereolithography-based 3D bioprinting system using visible light crosslinkable bioinks, Biofabrication 7 (2015), 045009, https://doi.org/10.1088/1758-5090/7/4/045009.
[148] R. Gauvin, Y.C. Chen, J.W. Lee, P. Soman, P. Zorlutuna, J.W. Nichol, H. Bae, S. Chen, A. Khademhosseini, Microfabrication of complex porous tissue engineering scaffolds using 3D projection stereolithography, Biomaterials 33 (2012) 3824–3834, https://doi.org/10.1016/j.biomaterials.2012.01.048.
[149] M. Gou, X. Qu, W. Zhu, M. Xiang, J. Yang, K. Zhang, Y. Wei, S. Chen, Bio-inspired detoxification using 3d-printed hydrogel nanocomposites, Nat. Commun. 5 (2014) 3774, https://doi.org/10.1038/ncomms4774.
[150] B. Guillotin, A. Souquet, S. Catros, M. Duocastella, B. Pippenger, S. Bellance, R. Bareille, M. Rémy, L. Bordenave, J. Amédée j, F. Guillemot, Laser assisted bioprinting of engineered tissue with high cell density and microscale organization, Biomaterials 31 (2010) 7250–7256, https://doi.org/10.1016/j.biomaterials.2010.05.055.
[151] N. Jones, Science in three dimensions: the print revolution, Nature 487 (2012) 22–23, https://doi.org/10.1038/487022a.
[152] T. Billiet, M. Vandenhaute, J. Schelfhout, S. Van Vlierberghe, P. Dubruel, A review of trends and limitations in hydrogel-rapid prototyping for tissue engineering, Biomaterials 33 (2012) 6020–6041, https://doi.org/10.1016/j.biomaterials.2012.04.050.
[153] S.P. Grogan, P.H. Chung, P. Soman, P. Chen, M.K. Lotz, S. Chen, D.D. D'Lima, Digital micromirror device projection printing system for meniscus tissue engineering, Acta Biomater. 9 (2013) 7218–7226, https://doi.org/10.1016/j.actbio.2013.03.020.
[154] B. Hopp, Femtosecond laser printing of living cells using absorbing film-assisted laser-induced forward transfer, Opt. Eng. 51 (2012), 014302, https://doi.org/10.1117/1.oe.51.1.014302.
[155] F.R. De Gruijl, H.J. Van Kranen, L.H.F. Mullenders, UV-induced DNA damage, repair, mutations and oncogenic pathways in skin cancer, J. Photochem. Photobiol. B Biol. 63 (2001) 19–27, https://doi.org/10.1016/S1011-1344(01)00199-3.
[156] R.P. Sinha, D.P. Häder, UV-induced DNA damage and repair: a review, Photochem. Photobiol. Sci. 1 (2002) 225–236, https://doi.org/10.1039/b201230h.
[157] Y. He, F. Yang, H. Zhao, Q. Gao, B. Xia, J. Fu, Research on the printability of hydrogels in 3D bioprinting, Sci. Rep. 6 (2016) 29977, https://doi.org/10.1038/srep29977.